M 2014

U.PORTO
FEUP FACULDADE DE ENGENHARIA
UNIVERSIDADE DO PORTO

PLGA NANOPARTICLES AS A PLATFORM FOR VITAMIN D -BASED CANCER THERAPY

MARIA JOÃO ALVES RAMALHO
DISSERTAÇÃO DE MESTRADO APRESENTADA
À FACULDADE DE ENGENHARIA DA UNIVERSIDADE DO PORTO EM
MESTRADO EM ENGENHARIA BIOMÉDICA

FACULTY OF ENGINEERING OF UNIVERSITY OF PORTO

Master in Biomedical Engineering

PLGA Nanoparticles as a platform for Vitamin D - based cancer therapy

Maria João Alves Ramalho
meb12006

Dissertation for the degree
Master in Biomedical Engineering
Supervisor: Prof. Dr. Maria do Carmo Pereira
Co-supervisor: Prof. Dr. Manuel Coelho

Porto, July 2014

“'The scientist is not a person who gives the right answers; he's one who asks the right questions.”

Claude Levi-Strauss

ACKNOWLEDGMENTS

There are numerous people that contributed to this dissertation and for that I am grateful to all of them. First of all, I wish to acknowledge my supervisor and co-supervisor; Prof. Dr. Maria do Carmo Pereira and Prof. Dr. Manuel Coelho, for their valuable advice, corrections and suggestions.

To my lab colleagues, Joana and Silvia, thanks for their kind help and important work discussions, and in special to Bárbara for her tireless guidance on my first contact with the lab, and to Manuela, for her valuable help on the cytotoxicity studies.

I must also gratefully acknowledge Rui Fernandes from IBMC for the TEM morphologic analysis of PLGA nanoparticles and Dr. Filipe Santos Silva for providing human pancreatic cell lines (hTERT-HPNE and S2-013) as for the possibility to use its facilities at the Institute of Molecular Pathology and Immunology of the University of Porto (IPATIMUP, Porto, Portugal). I would like also to thank to Andreia Sousa from IPATIMUP for always being available to help.

I would like to thank my colleagues and friends for their company as for their friendship. I would also like to thank João for his constant presence.

Last but not least, I am grateful to my parents, for their continuous support, encouragement words and wise advices.

I also gratefully acknowledge funding received from FCT-project (PTDC/QUI-BIQ/115449/2009).

ABSTRACT

Calcitriol, the active metabolite of Vitamin D_3, is a potential anticancer agent but exhibits several drawbacks as low bioavailability and high toxicity. Therefore, new therapeutic strategies, as specific drug delivery systems, must be developed in order to overcome those limitations. In this work, Vitamin D_3 metabolites were encapsulated in poly(lactide-co-glycolide) nanoparticles (PLGA NPs). PLGA nanoparticles with controlled sizes and properties, as nanocarriers of cholecalciferol and calcitriol, were prepared using the single emulsion-solvent evaporation technique. Two formulation parameters, vitamin/polymer ratio and sonication time, were studied and discussed using cholecalciferol as a drug model. After synthesis, the PLGA NPs with and without Vitamin D were analyzed in terms of size, shape and zeta potential. The attained systems for calcitriol showed mean diameters smaller than 200 nm, encapsulation efficiency of 57%, a loading capacity of approximately 6% and a process yield of 57%. The PLGA NPs remained stable at storage conditions for several weeks and they were lyophilized to increase their shelf-life. Studies on calcitriol release from the PLGA NPs have shown a biphasic pattern with an initial burst release, attributed to the surface-adsorbed vitamin, followed by a slower controlled release, correspondent to the calcitriol entrapped inside the NPs' matrix. The cytotoxic effect of calcitriol encapsulated in PLGA NPs was evaluated on two human pancreatic cells lines, hTERT-HPNE and S2-013. The *in vitro* studies demonstrated that bare PLGA NPs are biocompatible and the antineoplastic effect of calcitriol against human pancreatic cancer cells is enhanced by the nanoparticle formulation in terms of cell survival and growth. From the attained results, it was possible to conclude that PLGA NP formulation is a suitable nanocarrier for vitamin D_3 active metabolites, since they are able to improve therapeutic efficiency and potentially reduce calcitriol toxic effects in normal tissues.

Keywords: PLGA Nanoparticles, Poly(lactide-co-glycolide), Vitamin D_3, Calcitriol, 1,25 Dihydroxyvitamin D_3, Cancer Therapy, Drug Delivery, Nanocarrier

CONTENTS

LIST OF FIGURES

LIST OF TABLES

LIST OF ABBREVIATIONS

Calcidiol - [25-OH-D3])

Calcitriol - [1,25-(OH)2D3]

DBP - Vitamin D Binding Protein

DDS - Drug Delivery Systems

DLS - Dynamic Light Scattering

DMEM - Dulbecco's Modified Eagle medium

DMSO - Dimethyl sulfoxide

EE - Encapsulation Efficiency

ELS - Electrophoretic Light Scattering

EPR effect - Enhanced Permeability and Retention effect

FBS - Fetal Bovine Serum

FDA - Food and Drug Administration

GI_{50} - Half maximal growth inhibitory concentration

IC_{50} - Half maximal survival inhibitory concentration

LC -Loading Capacity

MDR - Multi-drug Resistance

MW – Molecular weight

NP(s) – Nanoparticles(s)

PBS - Phosphate Buffered Saline

PdI - Polydispersitivity Index

PEG - Polyethylene Glycol

PGA - Poly Glycolic Acid

PLA - Poly Lactic Acid

PLGA - Poly(lactic-co-glycolic acid)

RGD -Tripeptide Arg-Gly-Asp

RH - Hydrodynamic Radius

SD – Standard Deviation

SRB - Sulforhodamine B

TCA - Tricloroacetic Acid

TEM - Transmission Electron Microscopy

UV-Vis – Ultraviolet–Visible radiation

VDR - Vitamin D Receptor

ζ –potential – Zeta Potential

1 INTRODUCTION

1.1 Motivation

Cancer is the main cause of death worldwide. Despite the advances in medicine and technology fields, the aging and increase of the world's population has led to a raise in cancer incidence [1]. Although chemotherapeutic agents are effective in cancer treatment, their success is largely hindered as a result of acting indiscriminately on both tumor and healthy tissues, inadequate accessibility of antineoplastic agents to tumor tissue, requiring high doses, rapid abolition, poor solubility and inconsistent bioavailability [2]. In more recent years, Vitamin D_3 exhibited a major role in tumor's pathogenesis, progression and therapy [3]. Although as other chemotherapeutic agents, the use of Vitamin D_3 also exhibits several drawbacks. These limitations are recently leading to numerous investigations in order to design and develop an ideal formulation for Vitamin D_3 delivery to cancer cells.

A growing effort has being applied to find novel approaches for cancer treatment and in recent years a growing number of studies, focused on the research and development of nanoparticles as drug delivery systems, have been conducted. For that purpose, the nanosystem must meet several requirements such as biocompatibility, biodegradability, mechanical strength, FDA- approved and process synthesis low complexity. Nowadays, one of the most attractive candidates is Poly(lactide-co-glycolide)(PLGA), which is a co-polymer of poly lactic acid (PLA) and poly glycolic acid (PGA) [4-6]. As the success of a cancer therapy depends not only on the pharmacokinetic and pharmacodynamic activity of the therapeutic agent, but to a large extent, on its bioavailability and toxicity [4], the development of a nanocarrier for Vitamin D will allow to enhance its anti-cancer activity.

1.2 Main objectives

The main aim of the present work is to develop a suitable PLGA-based nanocarrier for vitamin D active metabolites, and evaluate the capacity of this polymeric system to improve therapeutic efficiency and reducing toxic effects. For that purpose, PLGA nanoparticles with controlled sizes and properties were prepared in this study, as nanocarriers of cholecalciferol and calcitriol. Their synthesis was complemented with physicochemical characterization of structure and properties as well as the evaluation of their effect on two human pancreatic cells lines, hTERT-HPNE and S2-013. Although some studies, among Vitamin D_3 encapsulation, have been conducted, the use of PLGA nanoparticles for Vitamin D_3 delivery towards cancer treatment was never reported.

1.3 Thesis organization

This dissertation is organized into five chapters. This chapter, “Introduction”, presents the subject and main objectives of this research work. Chapter 2, “State of the art”, presents an overview of the Vitamin D_3 metabolites and PLGA nanoparticles, as also a review on the studies that have been developed so far on the Vitamin D_3 delivery. Chapter 3, “Materials and methods” focus on the main materials and methodologies used in this experimental work. On chapter 4, “Results and Discussions”, the attained results and respective discussion for the Vitamin D_3-loaded PLGA nanoparticles characterization and evaluation are presented. Finally, an overall summary about this study, its main conclusions and some future work perspectives are presented on Chapter 5, “Concluding remarks and future perspectives”.

2 STATE OF THE ART

2.1 Classic cancer therapy challenges

Cancer is considered the 21st Century's disease being one of the main causes of death worldwide. Despite the advances in medicine and technology fields, the aging and increase of the world's population has led to a raise in cancer incidence. In fact, the last statistic study carried out by GLOBOCAN project, in 2008, state that about 12.7 million cancer cases and 7.6 million cancer deaths are estimated to occur per year [1]. This sort of studies allows adopting the most suited strategies to improve cancer treatment and to focus on prevention, early diagnosis and more effective therapies. Surgery, radiotherapy and chemotherapy are the most used cancer therapies. Surgery and radiotherapy are examples of local therapies. Moreover, chemotherapy is considered as a systemic therapy, which enters the bloodstream and destroy or control cancer cells. Chemotherapy is probably the most common treatment, however chemotherapeutic agents are not able to differentiate between healthy and tumor tissue and so will act on tissues without discrimination, resulting in devastating side-effects. Among these are increased susceptibility to infections, fertility problems and healthy tissues destruction. Concluding, although chemotherapeutic agents are effective in cancer treatment, their success is largely hindered as a result of the inadequate accessibility of antineoplastic agents to tumor tissue, lack of specificity, requiring high doses, rapid abolition, poor solubility, devastating side effects and inconsistent bioavailability [2, 7]. Therefore, the continuous research for an ideal therapy is very important. In fact, nanomedicine can bring an important contribution in this search.

2.2 Nanoparticles as Drug Delivery Systems for cancer therapy

Nanotechnology has proven to be extremely advantageous in creating breakthroughs in diagnosis, treatment and monitoring of cancer, enabling early diagnosis and the controlled delivery of drugs [8]. In fact, a growing number of studies focused on the research and

development of nanoparticles as drug delivery systems (DDS) has been published. Nanoparticles are colloidal carriers with dimensions on the nano scale (10^{-9}m) with unique physicochemical properties as small size, larger surface area, stability, varied composition, biocompatibility and biodegradability [7, 9].

Encapsulating drugs in a nanocarrier has the following main objectives: to increase drug's bioavailability and bioaccumulation in the target site, and decrease drug's toxicity. The fulfillment of these main goals allows maximizing therapeutic effects and minimizing side effects. These goals are achieved by drug encapsulation itself, but also by modifying NPs' surface. The encapsulation of the drug minimizes premature degradation after administration, since it allows protection and stabilization of the drug against environmental factors. This drug increased stability ensures enhanced bioavailability. Also in order to increase the bioavailability of the drug, the functionalized NP allows overcoming the biological barriers that would lead to its elimination. The toxicity of the drug is also reduced since NPs allows the use of lower doses, since the delivery is localized rather than systemic. Also a decrease in toxicity is due to drug being less likely to act on healthy cells, since it is possible to direct NP to the diseased tissues, increasing accumulation in the target tissues.

NPs benefit from tumor's environment through passive targeting. The size of the drug-loaded NP alone is bigger than the free form of the drug. This brings an advantage in using NPs to cancer therapy due to increased Enhanced Permeability and Retention effect (EPR effect) of such tissues. As it is illustrated in figure 1, tumor tissues exhibit an increased permeability of blood vessels, while lymphatic drainage is decreased. This leads to an increase in the concentration of drug-loaded nanoparticles in the tumor tissue [10, 11]. However the vessels permeability is not homogeneous and a more selective approach needs to be used for NPs drug delivery treatment. As this EPR effect is not verified in healthy tissues, NPs permeability is hampered. Also DDS that depends only on passive targeting mechanisms are specificity-limited. Therefore active targeting strategies should be developed [7].

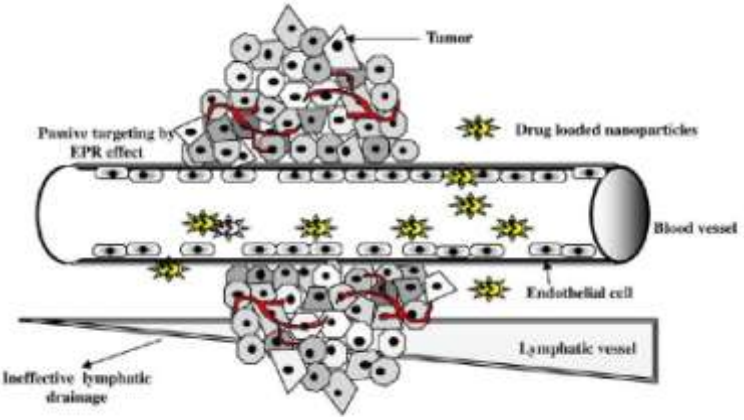

Figure 1 | Representation of the EPR effect in tumor tissue [4].

Ideally, for therapeutic use NPs should remain in circulation during the appropriate time, to be present at the target site in adequate amounts and improve the therapeutic efficacy. To be as efficient as possible, NP should meet certain requirements as being non-invasive, easy to prepare, economically viable and clearly a small and controlled size. If their surface is charged, the stability will be enhanced, due to the repulsion between them that hinders aggregation. NPs also must have a high loading capacity to allow carrying a large amount of drug [2, 12-14]. The efficiency of a therapeutic system for cancer's treatment is evaluated by its ability to reduce and destroy tumor cells minimizing the damage of the healthy tissues. This is where is highlighted the major contribution of NPs as nanocarriers of anticancer drugs, as they enable a targeted distribution into specific tissues [15]. Also NPs allow maintaining active doses of the drug for long periods of time, due to their controlled and sustained release. Another main goal of the use of NPs is that it is possible to address a specific therapy for each patient using tumor cell markers specific to each individual. The functionalization of the NP with these markers will result in a much more efficient therapy [10].

Currently, the most studied NPs for cancer nanotherapy are liposomes, polymeric and lipidic NPs, dendrimers, micelles, carbon and silica nanotubes (figure 2). However, although the extensive research, liposomes, lipidic and polymeric NPs are, at the moment, the only FDA-approved and clinically available formulations for cancer treatment [11]. Table 1 summarizes the commercially available nanoparticle-based therapeutic products for cancer therapies.

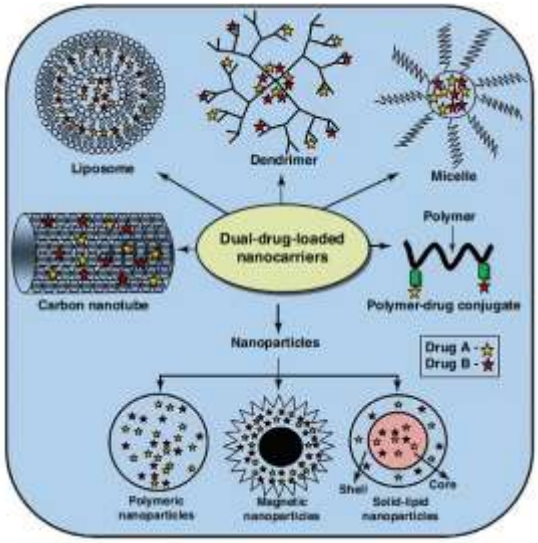

Figure 2 | Representation of different types of nanocarriers for drug delivery [11].

Table 1 | Clinically approved nanoparticle-based cancer therapeutics.

Trade name	Pharmaceutical Company	Composition		Indication	Administration route	FDA approval date	References
		Nanocarrier	Drug				
[(1)] Doxil ®	Ortho Biotech	Pegylated-Liposome	Doxorubicin	Refractory Kaposi's sarcoma, metastic breast and ovarian cancer	Intramuscular injection	Nov, 1995	[15-19,21]
[(1)] Caelyx®	Schering Plough	Pegylated-Liposome	Doxorubicin	Refractory Kaposi's sarcoma, metastic breast and ovarian cancer	Intramuscular injection	Nov, 1995	[15-19,21]
DaunoXome®	Diatos/Gilead Sciences	Liposome	Daunorubicin	HIV-related Kaposi's sarcoma	Intravenous injection	April, 1996	[15-19,21]
DepoCyt®	SkyePharma	Liposome	Cytarabine	Lymphomatous meningitis	Intrathecal injection	April, 1999	[16,18,21]
Lipusu®	Luye Pharma Group	Liposome	Paclitaxel	Metastatic ovarian and breast cancer; Lung cancer patients who cannot be treated with operation or radiotherapy	Intravenous injection	Only approved in China	[20]
Myocet ™	Zeneus Pharma/Elan Pharmaceuticals	Liposome	Doxorubicin	Metastic breast and ovarian cancer, and Kaposi's sarcoma	Intravenous injection	Only approved in Europe and Canada	[15-16,18-19,21]
Abraxane®	Abraxis Bioscience	Albumin-bound nanoparticles	Paclitaxel	Metastatic breast cancer; Lung cancer patients who cannot be treated with operation or radiotherapy	Intravenous injection	Jan, 2005	[15-16,18-19,21]
Genexol ® -PM	Samyang	Pegylated-PLA	Paclitaxel	Metastatic breast cancer; Lung and pancreatic cancer	Intravenous injection	Only approved in South Korea; Currently is on phase II in the USA	[16,21]
Nanoxel®	Dabur Pharma	Pegylated-PLA	Paclitaxel	Metastic breast and ovarian cancer, and Kaposi's sarcoma	Intravenous injection	Only approved in India	[22]
Oncaspar ®	Enzon	Polyethylene glycol	L-asparaginase	Acute lymphoblastic leukemia	Intravenous or intramuscular injection	Feb, 1994	[16,19,21]

Table prepared based on the following references: [15-22]. [(1)] Pegylated liposomal doxorubicin is known as Doxil® only in USA, and it is known as Caelyx® elsewhere.

2.2.1 PLGA Nanoparticles

Suitable nanomaterials for drug delivery must meet several requirements such as biocompatibility, biodegradability, mechanical strength, FDA- approved and process synthesis low complexity. One of the most attractive candidates is Poly (lactide-co glycolide)acid (PLGA), which is a co-polymer of poly lactic acid (PLA) and poly glycolic acid (PGA) linked by ester bonds as it is shown is figure 3 [4-6]. Although constituted by natural monomers, this is a synthetic polymer. Its adjustable biodegradation rate, strength and tunable mechanical properties justify its growing popularity. Also, its special features allow protection of drug from degradation and sustained release delivery [5].

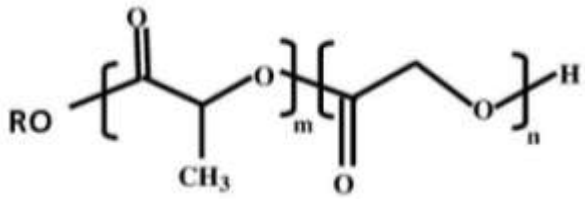

Figure 3 | Chemical structure of poly lactic-co-glycolic acid. m represents the number of lactic acid units and n is the number of glycolic acid units.

Biodegradability is a main feature of PLGA, since it can be used without the need for a surgical procedure to remove it [5]. It is well established that PLGA biodegradation occurs by hydrolytic cleavage of its esters linkages into monomers, glycolic and lactic acid [4-6, 23-27]. The degradation mechanism and reaction products of PLGA hydrolysis are represented in figure 4.

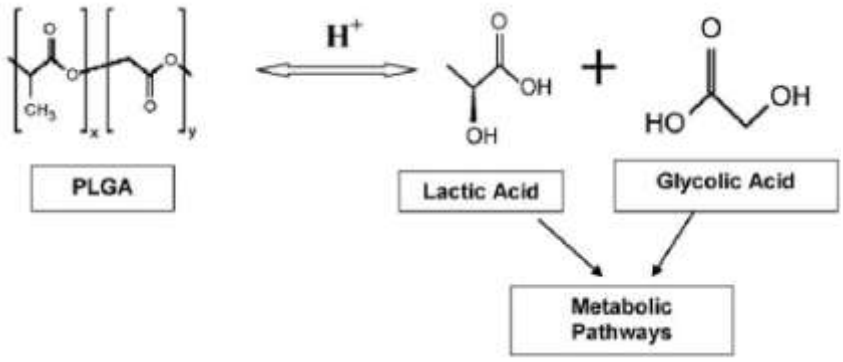

Figure 4 | Representation of hydrolytic degradation of PLGA and its products [6].

During hydrolysis the increasing number of free carboxylic end-groups lead to matrix swelling and increasing of hydrophilicity which enhances water-uptake [25]. These acidic products accumulate inside the PLGA NPs and are responsible for reaction auto-catalysis [25, 26]. The hydrolytic breakdown also causes the formation of pores in the matrix of the

polymeric system [23]. Many factors have been associated with the PLGA tunable degradation rate, such as: drug loading and type, polymer average molecular weight, polymeric molecular weight distribution, ratio of lactide to glycolide, effect of pH, porosity, cristalinity of the co-polymer [5, 23, 25-27].

Since PLGA decomposition products can be eliminated from the body by metabolic pathways, such as via the citric acid cycle (Krebs cycle), or directly by renal excretion, there is a minimal systemic toxicity associated [6]. Figure 5 schematizes how these metabolites are eliminated.

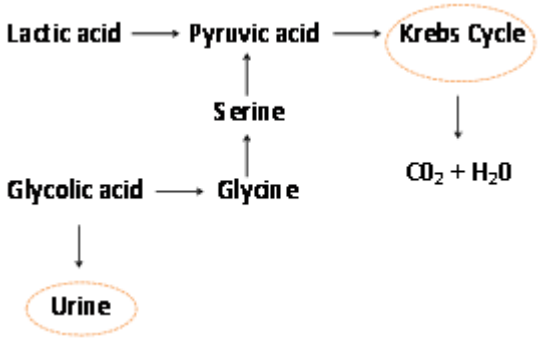

Figure 5 | Schematic representation of biological elimination pathways of PLGA biodegradation process. Lactic and glycolic acid enter the Krebs cycle and subsequently are eliminated from the body as carbon dioxide and water. In addition to this pathway, glycolic can also be excreted unchanged in the kidney. Adapted from: [6].

Although not causing tissue damages, PLGA NPs are not able to remain for a long time in blood stream because they are usually recognized by the immune system. Though, the size of the PLGA NP is extremely important with respect to blood circulation time [4]. If the system is smaller than 100 nm, the plasma protein adsorption to the NP surface is almost negligible, and the immune system is unable to eliminate NPs [27]. For NPs over 100 nm, their surface must be functionalized with biomolecules to increase blood circulation half-life. One of the most used strategies is coating their surface with a biodegradable copolymer with hydrophilic characteristics such as polyethylene glycol (PEG) [24]. However, passive targeting by choosing the size is not always sufficient in order to direct NPs to target tissues. To target cancer cells, several functionalized PLGA systems can be produced to enhance drug accumulation in the target area, recognition and binding to the target cell or tissue. For example, it is possible to modify their surface with folate, RGD, transferrine or specific antibodies [24, 28, 29].

Once they are recognized, PLGA NPs enter the target cell through receptor-mediated endocytosis. The acidic medium of late endosome triggers a charge change in PLGA NP. The NP becomes cationic leading to destabilization of late-endossomal membrane allowing efflux of NP and drug release, as it is shown in figure 6. Endosome-lysosome pathway is characterized by two types of compartments, the endosome and lysosome. Lysosomes are usually regarded as the terminal degradation compartment of this pathway. One important feature of PLGA NPs

is that they are cationic only in the endosomal compartment and do not destabilize the lysosomes, unlike another kinds of NPs. This allows to reduce their toxicity [4]. Another major advantage in the use of PLGA NPs is their ability to avoid the recognition of the P-glycoprotein, which is one of the main cells' drug resistance mechanisms [30].

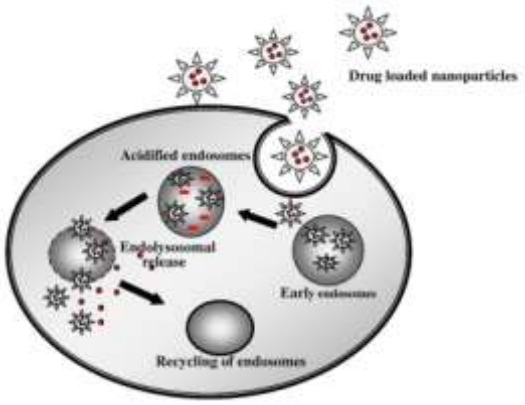

Figure 6 | Image illustrating PLGA NP endolysosomal efflux and drug release [4].

As the amount of encapsulated drug depends upon the drug's chemical structure and its interactions with PLGA [6], also several factors affect the PLGA NPs' release profile such as: (1) physico-chemical properties of the encapsulated drug; (2) geometry of drug-loaded PLGA NPs (size and shape); (3) drug solubility; (4) loading efficiency [6, 23, 26]. The main pathways for drug release in PLGA NPs are: (1) desorption of drug bound to the surface, (2) diffusion through NP matrix, (3) NP matrix hydrolysis,(4) or a combined degradation-diffusion process [5, 6, 23, 26]. PLGA NPs generally exhibit a biphasic release profile, characterized by an initial burst due to the release of surface-adsorbed drugs; followed by a biodegradation-accelerated release until complete polymer solubilization [6, 25]. This final phase is a combination of biodegradation-diffusion process [25]. Since adverse side effects of anti-cancer drugs are associated with high doses, this release pattern of PLGA NPs will allow a reduction of toxicity. This controlled and sustained release prevents high doses accumulation. Also, these slow release allow diminishing administration frequency, since drug levels are maintained over long periods of time [6].

PLGA NPs can be produced using several techniques. The characteristics of the obtained NP, as size and structural organization, depend upon the chosen method and solvents [5, 31, 32]. The most common methods are single or double-emulsion solvent evaporation and nanoprecipitation [6]. While nanoprecipitation is suitable for the entrapment of both hydrophobic and hydrophilic drugs [33], the choice of single or double emulsion

depends upon the hydrophilicity of the drug to be encapsulated [5]. Single-emulsion is a suitable choice for encapsulating hydrophobic drugs, and double-emulsion is mostly used for hydrophilic drugs [5, 32]. In nanoprecipitation method a precipitation of a dissolved material as nanoscale particle occurs after exposure to a non-solvent that is miscible with the solvent [34]. In contrast, in solvent evaporation technique, particles are formed from submicron emulsion droplets when immiscible solvents are mixed [33].

The extensive research around PLGA and the many systems already available in the market testify for the great success of this biomaterial. Tables 2 and 3 presented below summarize some of the PLGA applications clinically available, as also some applications in development or clinical trial phases.

Table 2 | Commercially available PLGA based particles formulations.

Trade name	Pharmaceutical Company	Drug	Indication	Administration route	FDA approval date	References
Lupron Depot®	TAP Pharmaceuticals	Leuprolide acetate	Hormone-dependent cancers	Intramuscular injection	Jan, 1989	[25, 35]
Sandostatin LAR® Depot	Novartis	Octreotide acetate	Acromegaly	Intramuscular injection	Nov, 1998	[25, 35]
Somatuline® LA	Ipsen	Lanreotide acetate	Acromegaly	Subcutaneous injection	Aug, 2007	[25, 35]
Telstar®	Pfizer / Watson Pharmaceuticals	Triptorelin pamoate	Prostate Cancer	Intramuscular injection	June, 2001	[25, 35]
Vivitrol®	Alkermes Inc. / Cephalon Inc.	Naltrexone	Management of alcohol and opioid dependence	Intramuscular injection	April, 2006	[25, 35]
Nutropin Depot®	Genentech	Somatropin	Growth hormone deficiency	Subcutaneous injection	Dec, 1999	[25, 35]

Table prepared based on the following references: [25, 35].

Table 3 | Currently developed PLGA-based particles as drug delivery systems for the treatment of different pathologies.

Drug	Surface funcionalization	Indication	Development phase	Trade name	Pharmaceutical Company	References
Docetaxel	PEG	Various cancers	Phase I clinical trial	BIND-014	BIND Bioscience	[18]
FX005	-	Treatment of Pain in Osteoarthritis of the Knee	Phase II of clinical trial completed	FX005-PLGA	PharmaNet Sp.	[36]
Benzocaine	-	Pain relief	In vitro studies	-	-	[37]
Cisplatin	PMSA	Prostate cancer	*In vitro* studies	-	-	[38]
Dexamethasone	-	Arthritis and osteoarthritis	*In vitro* studies	-	-	[39]
Doxorubicin	-	Various cancers	Animal studies (rats)	-	-	[40]
Etoposide	-	Various cancers	Animal studies (mice and rabbits)	-	-	[41]
Gentamycin	-	Brucellosis	Animal studies (mice)	-	-	[42]
Insulin	-	Diabetes	Animal studies (rats)	-	-	[43]
Paclitaxel	PEG	Liver tumor	Animal studies (mice)	-	-	[44]
Rapamycin	EGFR	Breast Cancer	*In vitro* studies	-	-	[45]
Rifampicin	-	Tuberculosis	Animal studies (mice)	-	-	[46]

Table prepared based on the following references: [18, 36-46] . Note that PMSA stands for Prostate-specific membrane antigen, EGFR for epidermal growth factor receptor and PEG for polyethylene glycol.

Despite the fact that PLGA NPs are widely used in medical applications, their use faces a few limitations as their poor loading capacity. The burst release mentioned above can be another major pitfall since large amounts of drug is loss before reaching the target tissue, resulting in an efficacy loss of the DDS. Also, the many required steps for NP production such as centrifugation and dialysis are expensive and difficult to scale-up [32]. PLGA NPs also exhibit a size-dependent cytotoxicity. Small PLGA NPs may trigger the generation of reactive oxygen species, mitochondrial depolarization and inflammatory cytokines release. However, some studies indicate that PLGA NPs larger than 100 nm would be safer for biomedical applications [47]. Another drawback of these polymeric NPs is the challenge of hydrophilic drugs entrapment, since those drugs rapidly partition into the aqueous phase during NPs preparation. For that is necessary to use appropriate preparation methods as the double emulsion technique [5]. Finally, it is essential to functionalize the NP surface in order to achieve a maximum efficacy [24].

2.3 Vitamin D_3 and its application in chemotherapy

Vitamin D, a seco-steroid hormone, is known as an important regulator of calcium homeostasis and bone mineralization [48-50]. However, in the late 1970s Vitamin D was found

in tissues not previously considered targets of vitamin D action, which came to disclose that this hormone may carry out several other functions, namely antineoplastic activity [51]. In humans' bloodstream, Vitamin D displays two main chemical forms: D_2 or ergocalciferol, and D_3 or cholecalciferol [52]. The first one comes from dietary source and the latter is produced in the epidermis from the action of sunlight and represents 95% of total blood's Vitamin D [52]. These two forms exhibit chemical differences in their side chains. As it is shown in figure 7, D_2 has an extra methyl group at C24 and an extra double bond between C22 and C23. These structural changes, between D_2 and D_3, are reflected in their affinity for the carrier known as vitamin D binding protein (DBP). Despite their metabolites' biologic activity is comparable, the fact that Vitamin D_3 has a higher affinity for DBP leads to the observation that in humans vitamin D_3 potency is three times higher than vitamin D_2's [53-55]. In fact, all evidence reported to date on the efficacy of vitamin D for cancer prevention has been based on vitamin D_3 [56]. For that reason only Vitamin D_3 will be covered for the next sections of this assay.

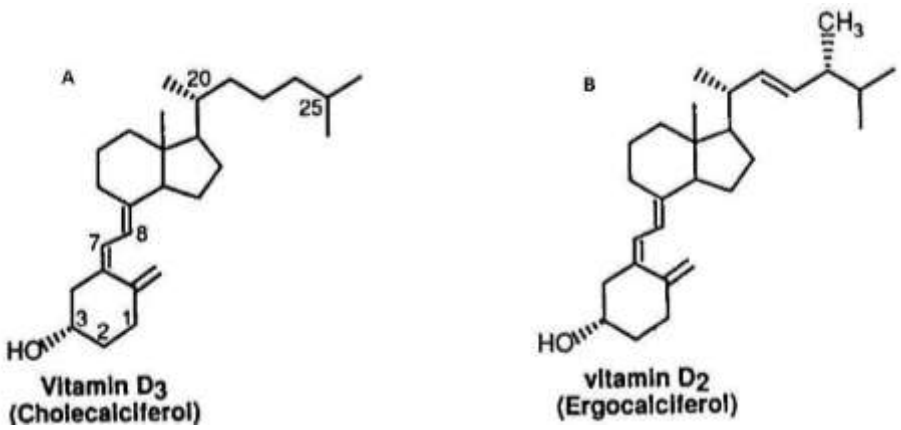

Figure 7 | Chemical structures of (A) Cholecalciferol and (B) Ergocalciferol [51].

Depending on its degree of hydroxylation, Vitamin D_3 can be found with three different chemical structures: Calciol, Calcidiol (25-OH-D3) and Calcitriol (1,25-$(OH)_2$D3). Cholecalciferol (Calciol) is inert and must be metabolized in the liver and the kidney through two hydroxylation processes to be converted to its active form, calcitriol [4]. In figure 8 it's schematized the structural formulas and the overall process of Vitamin D activation.

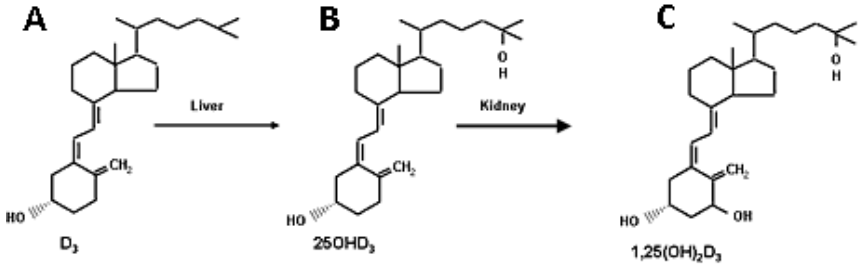

Figure 8 | Representation of Vitamin D_3 three different chemical structures: (A) Calciol; (B) Calcidiol; (C) Calcitriol. This scheme also represents the overall chemical reactions involved in the activation of Vitamin D [53].

Despite its well-known regulation of calcium homeostasis and bone mineralization functions, calcitriol is nowadays associated with many additional activities including anti-proliferative, pro-differentiating, anti-inflammatory, and immunomodulatory effects. For example, this hormone has the ability to suppress prostaglandin actions and enhance pro-inflammatory cytokines production, displaying a role in ceasing inflammatory process [57]. In figure 9 is summarized the vitamin's metabolism, as also calcitriol role in many biological functions [58].

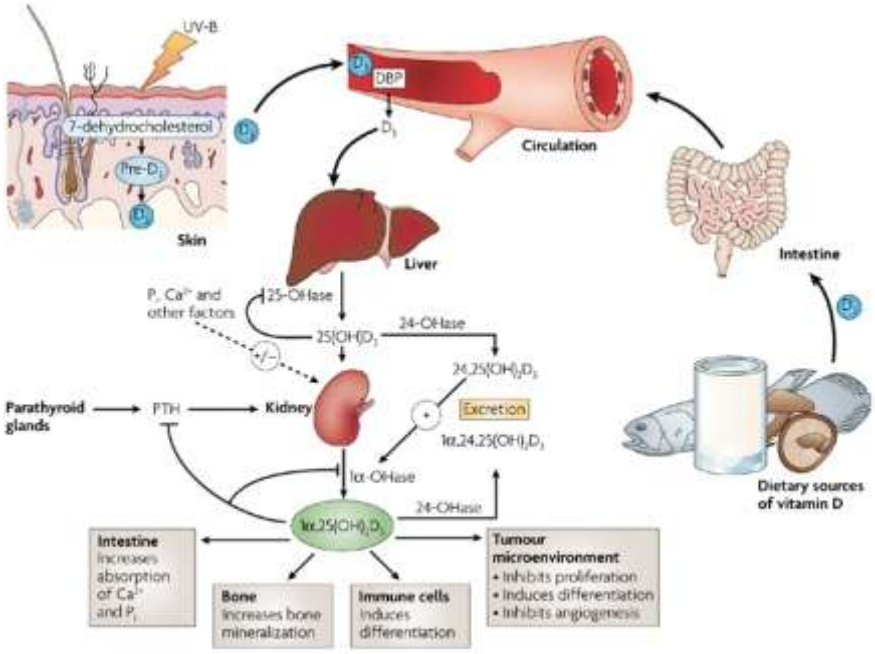

Figure 9 | Representation for epidermal synthesis of cholecalciferol, its metabolism and a multitude of its several potential physiological activities [58].

Several studies support that Vitamin D also plays a major role in tumor's pathogenesis, progression and therapy [3, 57, 59, 60] and the antineoplastic activity of calcitriol in pancreatic cancer is well established, as several *in vitro* and *in vivo* studies have been reported [61-64]. Calcitriol acts like classical steroid hormones, binding to vitamin D receptor (VDR) and targeting gene expression via both genomic and non-genomic pathways [3]. This receptor is widely distributed among tumor cells, regulating calcitriol antineoplastic activity [53, 57, 60]. Therefore several pathways by which vitamin D metabolites may prevent, treat or stop tumor growth have been described. The most discussed mechanisms are: (1) inhibition of tumor cell growth; (2) inhibition of angiogenesis and tumor metastasis; (3) triggering apoptosis; (4) enhancing "traditional" anticancer agents therapeutic action; (5) anti-inflammatory effects [3, 57, 59, 60]. A more detailed explanation about these mechanisms is presented below.

(1) VDR activation by calcitriol can inhibit tumor cell proliferation by inducing cell cycle arrest in the G_1/G_0 phase [3, 57, 59] or through inducing malignant cells differentiation in a variety of cell lines [57, 59, 60]. Calcitriol up-regulates the expression of the cell cycle inhibitors p21 and p27 leading to cell cycle arrest prior to DNA replication in S phase essential to cell division [65].

(2) Calcitriol also inhibits angiogenesis by reducing the proliferation of vascular endothelial cells [57, 59] and regulating the expression of key molecules, such as serine proteinases, metalloproteinases, extracellular matrix proteins and integrins [57, 60]. Another calcitriol antineoplastic activity is related to reducing the invasive and metastatic potential of tumor cells [3, 57, 60]. Inhibition of tumor metastasis is due to increased expression of E-cadherin, a tumor suppressor associated with the metastatic potential of cells, and inhibition of angiogenesis itself [60].

(3) Apoptosis triggering of tumor cells occurs through activation of the intrinsic pathway of apoptosis by increasing the expression of pro-apoptotic proteins and decrease the expression of anti-apoptotic proteins, or by directly activate effector caspases [3, 59]. Apoptosis may also be induced by inhibition of telomerase enzyme [59]. This programmed cell death is characterized by causing the disruption of mitochondrial function, cytochrome release and production of reactive oxygen species [3, 59].

(4) Vitamin D can also potentiate the antitumor actions of a number of more “traditional” anticancer agents [57, 59].

(5) Inflammatory mediators such as cytokines, chemokines, prostaglandins, and reactive oxygen and nitrogen species enhance tumorigenesis through the activation of multiple signaling pathways in tumor tissue. Hence, anti-inflammatory effect of calcitriol mentioned at the section above can be also considered as an antineoplastic activity [3, 57].

2.3.1 Nanoparticles as carrier for Vitamin D

Despite calcitriol’s multiple medicinal benefits, its low bioavailability and high toxicity continue to be highlighted as major challenges in developing formulations for clinical use. In fact, two pharmaceutical formulations for Rocaltrol® (registered trademark of Roche Pharmaceuticals) are available with different administration pathways, oral and intravenous, for the treatment of refractory malignancies. However, they are inappropriate for cancer treatment due to several technical issues, as the difficulty to maintain active systemic levels

[66, 67]. To overcome some of these limitations, drug delivery systems can be envisaged for new calcitriol formulations. Although several studies, among Vitamin D_3 encapsulation for food fortification, have been conducted, the use of nanocarriers for Vitamin D_3 delivery towards cancer treatment was only report three times. Two works intended Vitamin D_3 vectorisation in order to ensure specific action on malignant cells avoiding side effects as hypercalcemia. For that purpose, Nguyen and colleagues (2007) developed a formulation based on poly(vinyl neodecanoatecrosslinked-ethyleneglycol dimethacrylate) microspheres, with a size of approximately 35 µm. In this project cholecalciferol was used as a model drug for calcitriol. Nguyen and co-workers demonstrated that their cholecalciferol-loaded microspheres are biocompatible, allow controlled and sustained release and increase the efficiency of the therapy [68]. A few years later, Almouazen and partners (2012) developed a formulation using PLA nanoparticles with approximately 200 nm. This study proved that PLA nanocapsules are a suitable choice for controlled delivery of antineoplastic agents. Almouazen and co-workers also concluded that nanoencapsulated calcidiol induced a significant growth inhibition when compared to free calcidiol, and also that PLA NPs are able to enhance the intracellular delivery of vitamin on breast cancer [66]. Lastly, Bonor and co-workers (2012) developed calcitriol conjugated quantum dots (QD) to analyze calcitriol distribution and dynamics in mouse myoblast cell line. According to their conclusion, QD can be used for imaging drug-tumor interactions and to deliver drugs to tumors and metastasized sites [69].

Vitamin D_3 encapsulation in PLGA NPs, as intended in this work, should increase calcitriol bioavailability and reduce its toxicity. Several studies indicate that more than 75% of Vitamin D intake is catabolized and excreted before being converted to its active form or before its storage [52]. This fact could be a good reason to the use of NPs as drug delivery systems. Since these systems will prevent vitamin D elimination before the appropriate time, increasing vitamin's bioavailability. Vitamin D entrapment in PLGA NPs will also avoid first-pass effect suffered by orally ingested vitamin. After being absorbed by the intestinal mucosa, vitamin D is conducted by the portal vein to the liver where it is metabolized. Hepatic 24-hydroxylase enzyme inactivates calcitriol by hydroxylation. Therefore, vitamin D concentration is greatly reduced before it reaches the systemic circulation, and consequently reaches target tissues [70]. However, Vitamin D encapsulation in PLGA NPs could inhibit this degradation. Also should allow circumventing the multi-drug resistance (MDR) problem [30]. In addition to increasing the bioavailability, functionalization of PLGA NPs surface allow vitamin D vectorisation. This ensures specific action on cancer cells and increases the concentration delivered while avoiding side effects [6]. This specific-tissue targeting avoids hypercalcemia toxicity's phenomena. Calcitriol has anti-tumoral activity in supraphysiological dose (10^{-9} to

10^{-6} M *in vitro* and $>10^{-9}$ M *in vivo*) associated with a high risk of hypercalcemia [60, 66]. Finally, the characteristic drug release pattern already mentioned of this kind of NPs is a major advantage. PLGA NPs allow maintaining a controlled and sustained release of drugs. As in cancer, it is advantageous to have slow doses for long periods of time these NPs are a suitable choice, enhancing therapeutic efficiency. Low doses are related to less side-effect to healthy tissues. And also, sustained release allows diminishing the administration frequency since it allows maintaining active doses for longer periods of time [4].

3 MATERIALS AND METHODS

3.1 Materials

PLGA Resomer® RG503H (50:50; MW 24.000 – 38.000), ethyl acetate, Pluronic® F127 and phosphate buffered saline (PBS) were purchased from Sigma–Aldrich (St. Louis, Mo., U.S.A). Two aqueous solutions of 0.1% and 1%(w/v) Pluronic F127, respectively, were prepared. Cholecalciferol (Vitamin D_3, MW 384.65, purity ≥ 99%) was purchased from Alfa Aeasar (Karlsruhe, Germany). Calcitriol (Rocaltrol, MW 416.64, purity ≥ 99%) was purchased from Selleck Chemicals (Munich, Germany) and was reconstituted in 100% ethyl acetate and stored at -20 ºC. Ethanol [purity ≥ 99.9% (v/v)] was purchased from Carlo Erba Reagents (Val de Reuil, France). For TEM sample preparation, uranyl acetate (dehydrate, 424.146 g/mol) was purchased from Electron Microscopy Sciences (Hatfield, UK). For cytotoxicity assays, Dulbecco's Modified Eagle medium (DMEM) was obtained from Invitrogen Co. (Scotland, UK). Acetic acid, dimethyl sulfoxide (DMSO), sulforhodamine B (SRB) and trypan blue were purchased from Sigma-Aldrich (Germany). Tricloroacetic acid (TCA) and Tris buffer were acquired from Merck (Darmstadt, Germany). All aqueous solutions were prepared in deionized and filtered ultrapure Milli-Q water (Milli-Q Academic, Millipore, France).

3.2 Methods

3.2.1 PLGA nanoparticles preparation

PLGA NPs were prepared using the emulsion-solvent evaporation technique. There are two modifications of this process, the single and double emulsion. The choice depends upon the hydrophilicity of the drug to be encapsulated. As Vitamin D_3 metabolites are hydrophobic molecules, a single emulsion process was used [5, 31, 32]. For that purpose, 100 µL solution of 100 mg/mL of PLGA in ethyl acetate was prepared, and for encapsulation purpose 1 mg of vitamin was added. 200 µL of an aqueous solution of 1% (w/v) pluronic F127 was added dropwise to the organic phase (PLGA and vitamin dissolved in ethyl acetate). Then, the moisture was vortexed (Genius 3, ika®vortex, Germany) and emulsified by sonication at an

ultrasonic frequency of 45 kHz in a beaker with ice using Ultrasonic cleaner (VWR™, Malasya). Typically, stirring of the emulsion originates microdroplets. In order to induce the nanosized droplets, sonication process was carried out. The size reduction is induced through a two-step mechanism. Firstly, applying acoustic waves through the water creates interfacial waves and instability which causes the eruption of the oil phase into the water medium in the form of droplets. Secondly, applying low frequency ultrasound causes acoustic cavitation, that is, the formation and subsequent collapse of microbubbles, leading to turbulence. This turbulence breaks up the primary droplets of dispersed oil into nanosized droplets [71, 72].

After emulsification was completed, the emulsion was poured very fast into 2.5 mL of 0.1% (w/v) pluronic F127 and stirred (800 rpm) at room temperature for 3 hours in order to completely evaporate the organic solvent, using Colorsquid (ika®) magnetic stirrer. It is important to note that, this transfer step must be completed very quickly, in order to avoid PLGA NPs aggregation before being stabilized by the surfactant. The evaporation step was performed in a flow chamber Captair®bio from Erlab (Barcelona, Spain). Evaporation of the solvent transforms droplets of dispersed phase into solid particles [73].

The resulting suspension was filtered with Millex-GP Filter Units (0.2 µm, polyethersulfone) (Millipore Express, Ireland) and incubated at 4 ºC overnight to avoid NPs aggregation and increase their stability. Then the NPs were collected by centrifugation (14500 rpm, 30 min) with MiniSpin®plus (Eppendorf, Germany), and the pellet was resuspended in 1 mL of ultrapure water. The supernatant was also saved for analysis.

Two experimental parameters, the sonication step and the vitamin/polymer ratio, were tested in order to achieve the adequate experimental conditions. For sonication time, 1, 5 and 10 minutes were evaluated. Also, 1% and 10% (w/w) of vitamin were tested. Due to the cost of calcitriol, the inactive form of vitamin D_3, cholecalciferol, was used as drug model in this step. All formulations were prepared in triplicate.

In this described process, the drug is incorporated during the NP production. However, the drug could be adsorbed on the NP after its production [32].

3.2.2 PLGA Nanoparticles physicochemical characterization

The size, polydispersity index, zeta potential, morphological appearance and drug-loading capacity were the parameters used to characterize the produced nanoparticles. The effect of process parameters on nanoparticles properties was assessed, including different times of sonication and the vitamin/polymer ratio.

3.2.2.1 Nanoparticles size

Dynamic Light Scattering (DLS) is a well known technique to determine the size of nanoparticles in dispersion or solution. When a light beam hits on a NP, part of the incident light is scattered. As NPs in suspension are in constant movement due to Brownian motions, they lead to changes in scattered light intensity. Then, DLS can provide information about the average size and size distribution of a NP in suspension, by measuring the fluctuations of scattered light intensity as a function of time. The rate of change of scattered light is directly proportional to the movement of the particles and can be related to their diffusion coefficient. Then, NPs size can be calculated from the diffusion coefficient D, using Stokes-Einstein equation [74, 75]:

$$R_H = \frac{kT}{6\pi\eta D} \quad (1)$$

where, R_H is the hydrodynamic radius; k, the Boltzmann constant; T, temperature; η, the viscosity of the solvent.

In addition to the size, DLS also allows determining the polydispersity index (PdI). PdI is an indicative of the heterogeneity of NPs sizes in a suspension [75]. For a near-monodisperse sample, a PDI of 0.1 or lower is expected [76]. The presence of aggregates can distort the results, since the equipment analyzes them as a large size single particle, resulting in higher PdIs [77].

In this work, DLS measurements were performed using a ZetaSizer Nano ZS (Malvern Instruments, Worcestershire, UK). The size distribution was given by PdI. All the determinations were performed in disposable cells (Sarstedt, Germany) and using water as dispersant medium. Mean values for each preparation were obtained by triplicate measurements. Each measurement was performed with 12 runs.

3.2.2.2 Zeta Potential

Electrophoretic light scattering (ELS), also known as Laser Doppler Micro-electrophoresis, is used to evaluate the zeta potential (ζ –potential), a key parameter that controls electrostatic interactions between particles in a dispersion and therefore its stability [78]. Particles in a suspension attract ions to their surface. These ions form an electrical double layer covering the particle surface. This double layer comprises an inner layer, the Stern layer where counterions are strongly adsorbed; and an outer layer, where ions diffuse more freely. This diffuse layer terminates the boundary of the particle as a single charged entity and the

electric potential that exists at this boundary is called the zeta potential. Particles with very positive/negative ζ –potential will repel each other and resist to aggregation. On the contrary, low absolute zeta potential values results in aggregation and flocculation [79]. A physically stable nanosuspension will have a minimum zeta potential of absolute value of 30 mV [31].

When an electric field is applied, electrophoresis occurs and ELS measures the velocity of the charged particles [78]. Electrophoretic mobility (μ) is given by the following equation [80]:

$$\mu = \frac{v}{E} \quad (2)$$

where, *v* is the velocity; and *E*, the applied electric field.

Then, Henry's Law allows to calculate ζ-potential [78]:

$$\mu = \frac{2\varepsilon\zeta F(ka)}{3\eta} \quad (3)$$

where μ is the eletrophoretic mobility; ε, the dielectric constant of the dispersant; ζ, the zeta-potential; *F(ka)*, is the Henry function; and η, the viscosity coefficient.

Usually the laboratory equipments incorporate several techniques in a single compact unit. In fact, in this work ZetaSizer Nano ZS also provided measurements of zeta potencial by ELS. It was used folded capillary cells from Malvern (Worcestershire, UK) and the dispersant medium was water. Mean values for each preparation were obtained by triplicate measurements. Each measurement was performed with 12 runs.

3.2.2.3 Morphologic analysis

Transmission electron microscopy (TEM) is one of the most efficient and versatile tools for the characterization of nanomaterials morphology. This technique has much higher resolution than conventional light microscopy and is based on the interaction of an electron beam with the sample through which it passes. When the beam hits the sample, electrons interact with the matter, and part of them is transmitted through the sample. These transmitted electrons are focused to a phosphor screen at the bottom of the microscope where the image is formed. The beam that reaches the phosphor screen consisted of different amounts of electrons that pass through particular regions of the sample. This difference is responsible for the image contrast. Darker areas of the image represent the regions of the sample through which fewer electrons were transmitted, due to the greater thickness or density. Contrariwise, brighter areas are the result of increased electronic transmission through the sample, i.e. representing thin regions of the sample [81, 82].

The morphological examination of the NPs was performed by TEM Yeol Yem 1400 at an accelerating voltage of 80kV (Tokyo, Japan). For that purpose, the samples were prepared with negative staining. 10 µL samples were stained with 2% (v/v) uranyl acetate for 45 seconds, immobilized on copper grids (Formvar/Carbon on 400 mesh Cu (50) from Agar Scientific), and air-dried for TEM visualization [83]. TEM samples must be prepared in order to improve their visualization. Uranyl acetate is a heavy metal salt capable of scattering electrons, and therefore enhancing the image contrast [84].

3.2.2.4 Nanoparticles loading capacity

Cholecalciferol and calcitriol loading capacity (LC) of PLGA NPs was calculated by the following equation:

$$LC = \frac{total\ weight\ of\ drug - unloaded\ weight\ of\ drug}{total\ polymer\ weight}\ x\ 100 \qquad (4)$$

Loading capacity was determined indirectly. Therefore, the quantity of drug entrapped in the NPs was calculated by the difference between the total drug dissolved in ethyl acetate during NPs preparation and the quantity of non-entrapped vitamin remaining in the aqueous suspending medium. For the quantification of the free cholecalciferol and calcitriol, the NPs suspension was centrifuged (14500 rpm, 30 min), and the supernatant analyzed. The sample was measured by UV-Vis spectrophotometry at 265 nm, using a UV-1700 PharmaSpec UV-Vis spectrophotometer from Shimadzu (Japan). The results were correlated to a calibration curve for which vitamin form in 3.5% of ethyl acetate in an aqueous solution of 0.1% pluronic (Appendix A and B– figures 17 and 18). This step was conducted before organic solvent evaporation in order to ensure vitamin solubility. All experiments were performed in triplicate.

3.2.3 Determination of encapsulation efficiency

The quantification of cholecalciferol and calcitriol entrapped in the NPs was conducted as previously described in section 3.2.2.4. All experiments were performed in triplicate. Encapsulation efficiency (EE) of PLGA NPs was calculated by the following equation:

$$EE = \frac{total\ weight\ of\ drug - unloaded\ weight\ of\ drug}{total\ weight\ of\ drug}\ x\ 100 \qquad (5)$$

3.2.4 Determination of Process Yield

For the determination of the NPs production yield, the difference between the used polymer mass for the NPs preparation and the actual dried NPs weights were obtained. All experiments were performed in triplicate. The yield of the process was calculated by the following equation:

$$Process\ Yield\ (\%) = \frac{total\ nanoparticles\ weight}{polymer\ weigh}\ x\ 100 \qquad (6)$$

The unloaded NPs weight was determined by gravimetry following a procedure adapted from Grenha and co-workers [83]. The NPs suspension was centrifuged (14500 rpm, 30 min). The pellet NPs were resuspended in 200 µL of deionized water and the supernatant was discarded. The pellet was dried overnight, and the final mass of the NPs was measured. All experiments were performed in triplicate.

3.2.5 NPs stability studies

In order to evaluate the PLGA NPs stability, PLGA NPs' dispersions in ultrapure water were stored at 4 °C. These tests were performed in both formulations; cholecalciferol-loaded and calcitriol-loaded NPs. DLS and ELS measurements were performed to evaluate modifications in PLGA NPs size and zeta potential. These measurements were performed every week, over a period of nine weeks.

The drug-loaded PLGA NPs were re-suspended in ultrapure water (200 µg.mL^{-1}) into an eppendorf semi-capped to allow gas output during freeze-drying process. Samples were frozen at −20 °C for 3 hours and then lyophilization was carried out in a BenchTop^{TM} K series freeze-drier from VirTis® (NY, USA) at 5 x 10^{-5} Bar and – 95 ^{o}C for 48 hours. The freeze-dried samples were sealed and stored at 4 °C before analysis. The samples were then reconstituted within a day using the same initial volume (1 mL) of ultrapure water. Mean size variation and particle aggregation was quantified by DLS analysis. After the lyophilized cake hydration, the vitamin D

stability analysis was also performed by UV-Vis spectrophotometry measurements. All formulations were prepared in triplicate.

The effect of sucrose as a cryoprotective agent on the NPs stability during freeze-drying was also determined. The cryoprotectant was added to the drug-loaded PLGA NPs suspension before freezing at the concentration of 1% (w/v). All experiments were performed in triplicate.

3.2.6 *In vitro* release studies

In vitro release behavior of calcitriol entrapped in the PLGA NPs were assessed using a modified centrifugation method [85] over seven days. A sufficient amount of calcitriol-loaded PLGA NPs were re-suspended in release buffer (PBS 0.01 M, pH 7.4) and divided in 7 aliquots. The aliquots were maintained in a water bath at 37 °C in a drying oven (Venti-line, VWR, Belgium). At determined set time points, each aliquot was withdrawn from the water bath and centrifuged at 14400 rpm for 10 min. Amicon® Ultra-0.5 centrifugal filter devices (Millipore, County Cork, Ireland) were used in order to remove PLGA degradation products and NPs and then the release medium was freeze-dried. The lyophilized samples were further reconstituted with ethanol 100% (v/v) for measurement by UV-Vis spectrophotometry at 265 nm. The results were correlated to a calibration curve in ethanol (Appendix B – figure 19). The calcitriol release curve, representing the percentage of drug released in function of time, was then drawn by the following equation:

$$\%\ drug\ released = \frac{amount\ of\ drug\ released\ at\ time\ t}{amount\ of\ encapsulated\ drug}\ x\ 100 \qquad (7)$$

3.2.7 Cell lines

The two human pancreatic cell lines studied, T-HPNE (hTERT immortalized Human Pancreatic Nestin-Expressing normal ductal-derived epithelial cells) and S2-013 (well differentiated tubular adenocarcinoma and moderately metastatic subline cloned from the human pancreatic tumor cell line SUIT-2), were kindly provided by Prof. M. A. Hollingsworth (Eppley Institute for Research in Cancer and Allied Diseases, UNMC, Omaha, NE, USA) [86, 87].

For cell culture proposes, both cell lines were maintained in DMEM medium, supplemented with 10% fetal bovine serum (FBS) at 37 °C in a humidified 5% CO_2 incubator. When the cells reached 80% of confluence, they were trypsinized and subcultured.

3.2.8 *In vitro* cytotoxicity studies

The effects of the calcitriol-loaded PLGA nanoparticles and free calcitriol, on the cell growth and survival in pancreatic cell lines, were evaluated using Sulforhodamine B (SRB) assay. SBR assay is a colorimetric, sensitive, nondestructive, rapid and inexpensive assay that is used for the *in vitro* measurement of cellular protein content [88, 89]. Sulforhodamine B is an anionic bright pink aminoxanthene protein dye with two sulfonic groups [89]. SBR binds to basic amino acids of proteins of TCA-fixed cells. The colorimetric evaluation provides an estimate total protein mass, which is related to cell number and therefore related to cell survival and viability [88-90].

Experiments were performed in 96-well assay plates, where exponentially growing cells were seeded for an incubation period of 24 hours at a density of 1000 cells per well before treatment with free calcitriol, blank PLGA NPs and calcitriol-loaded PLGA NPs. This incubation period under normal conditions (5% CO_2 humidified atmosphere at 37 ºC) allows cell to adhere. The samples of NPs and free calcitriol were diluted in DMEM at eight final concentrations of calcitriol ranging from 5 to 2500 nM, and the cells were incubated with these samples for 48 h and 72 h, respectively. A calcitriol stock solution of 2.4 mM was prepared in ethanol to ensure calcitriol solubility in culture medium. However all samples of calcitriol alone contained at most 0.1% (v/v) ethanol. Due to the short half-life of calcitriol, the supplemented medium was renewed daily. After the 48–72 hours incubation period, the cytotoxic effect was assayed by SRB, using a well described methodology established by Skehan and colleagues (1990) [91]. The cells were fixated with 10% TCA for 1 hour on ice. After the incubation period the cell monolayers were washed and stained with 50 µL SRB dye for 30 minutes. The cells were then washed repeatedly with 1% acetic acid to remove unbound dye. The cells air-dried and the protein-bound stain was solubilised with 10 mM Tris solution. The SRB absorbance was measured at 560 nm using the PowerWave microplate reader (HT Microplate Spectrophotometer, BioTek).

The absorbance of the wells after incubation period were analyzed and compared by the following equations [92]:

- as measure of cell viability and survival in the presence of calcitriol-loaded PLGA NPs and free calcitriol:

$$(\%) = \frac{T}{C}\ x\ 100 \quad (8)$$

- as measure for growth inhibition in the presence of calcitriol-loaded PLGA NPs and free calcitriol:

$$(\%) = \frac{(T-T_0)}{(C-T_0)}\ x\ 100 \quad (9)$$

where T is the quantitative measurement (absorbance value) at the end of the incubation period in the wells containing loaded PLGA NP or free calcitriol, T_0 is the quantitative measurement at the time of test drug addition and C is the quantitative measurement in the control wells (untreated cells). Therefore, concentration-response curves using non-linear regression analysis were obtained and the concentration inhibiting cell survival by 50% (IC_{50}), together with the concentration inhibiting the net cell growth by 50% (GI_{50}) were determined. IC_{50} and GI_{50} are the concentrations of test drug where the following equations, respectively, are applicable [92]:

$$\text{For } IC_{50}: \frac{T}{C}\ x\ 100 = 50\% \quad (10)$$

$$\text{For } GI_{50}: \frac{(T-T_0)}{(C-T_0)}\ x\ 100 = 50\% \quad (11)$$

Bare PLGA NPs and 0.1% ethanol were added as control to assess if they will affect cell survival in control cells. Also, not exposed cells were also included in all assays as no-treatment controls (null controls) and all samples were tested in triplicates.

3.2.9 Statistical analysis

Statistical analysis was performed by using two-tailed Student's t-test, considering a confidence interval of 95%. P-values lower than 0.05 were considered significant.

4. RESULTS AND DISCUSSION

4.1 Physicochemical characterization of PLGA nanoparticles

PLGA NPs were prepared by a single emulsion solvent evaporation method and stabilized with Pluronic F127. Sonication of the emulsion is a crucial step to define the size of the nanoparticles. As stirring of the emulsion originates microdroplets, sonication process allows size reduction to nanoscale [71]. The influence of the sonication time was evaluated and the physicochemical properties of the produced unloaded PLGA NPs are presented in table 4.

Table 4 | Effect of sonication time on the physicochemical properties of the produced bare PLGA NPs. Data represented as mean ± SD (n=3).

	Sonication time	Mean diameter (nm)	PdI	Zeta potential (mV)
Bare PLGA NPs	1 min	176 ± 2	0.096 ± 0.090	- 34 ± 4
	5 min	172 ± 4	0.064 ± 0.040	- 38 ± 3
	10 min	173 ± 18	0.054 ± 0.027	- 36 ± 3

Typically, according to the literature, PLGA NPs size is founded to be in the range of 100 to 250 nm [32]. The unloaded NPs, produced with three different sonication times, exhibited mean sizes varying between 172 and 176 nm. It was concluded that with increased sonication time, mean sizes were not significantly different ($P>0.05$) and are within the expected range. Also, no significant changes were verified ($P>0.05$) for PdI and zeta potential values. The sonication time selected for the following experiments was 5 minutes.

The single emulsion solvent evaporation method allowed the encapsulation of vitamin D_3 in the PLGA NPs. The attained results for mean diameter, PdI, zeta potential, encapsulation efficiency and loading capacity values for the PLGA NPs loaded with cholecalciferol and calcitriol are shown in table 5.

Table 5 | Physicochemical features of cholecalciferol and calcitriol-loaded PLGA NPs. Data represented as mean ± SD (n=3).

	Vitamin D /polymer ratio	Mean diameter (nm)	PdI	Zeta potential (mV)	EE (%)	LC (%)
Cholecalciferol-loaded PLGA NPs	1%	172 ± 8	0.069 ± 0.033	- 33 ± 1	81 ± 17	0.8 ± 0.1
	10%	185 ± 6	0.133 ± 0.060	- 29 ± 4	83 ± 2	8.3 ± 0.2
Calcitriol-loaded PLGA NPs	10%	185 ± 4	0.052 ± 0.040	- 31 ± 1	57 ± 8	5.7 ± 0.9

As it can be concluded after the analysis of table 5, the mean diameters of the loaded PLGA NPs ranged from 172 to 185 nm. That is, they were according to the expected values. As it is also shown in tables 4 and 5, 10% drug-loaded NPs exhibited a significantly larger size than unloaded PLGA NPs ($P \leq 0.05$), regardless of whether it was encapsulated cholecalciferol or calcitriol. The size increased from 172 (± 4) to 185 (± 6) nm and 185 (± 4), respectively. This effect was reported in studies that argue that the drug causes an expansion of the polymeric matrix, increasing particle size [93]. This matrix expansion also explains the significant increase ($P \leq 0.05$) of the NP diameter as the choelcalciferol/polymer ratio increases, from 172 (± 8) in 1% cholecalciferol to 185 (± 6) nm in 10% cholecalciferol. Moreover, mean size values were not significantly different for both 10% cholecalciferol and 10% calcitriol-loaded NPs ($P > 0.05$). The prepared systems exhibited a narrow size distribution (PdI ≤ 0.1).

Zeta potential values for PLGA NPs are negative as expected, ranging from -38 to -29 mV, due to their carboxylic end-groups, as it is shown in tables 4 and 5. Zeta potential absolute value significantly decreased from 38 in unloaded PLGA NPs to 29 and 31 mV in 10% cholecalciferol-loaded and6 10% calcitriol-loaded NPs, respectively ($P \leq 0.05$). These values could be explained by Vitamin D adsorption on PLGA NPs surface. As already reported by Musumeci and colleagues, the drug adsorbed on PLGA NPs surface exert a masking effect of the superficial carboxylic groups, reducing the effective NP charge [93]. This masking effect could also explain the decrease, although not significant ($P > 0.05$), in zeta potential values when cholecalciferol proportion increased from 1 to 10%, since more available vitamin D may led to a greater adsorption at NPs surface. Moreover, zeta potential values were not significantly different for both 10% cholecalciferol and 10% calcitriol-loaded NPs ($P > 0.05$). NPs' stability is a result of static stabilization, i.e., electrostatic forces due to the PLGA carboxylate groups at the NP surface, and the surfactant behavior that also plays a crucial role in

maintaining nanosuspension stabilization. During particle formation, the stabilizer is able to modify NPs stabilization [59] by adsorbing onto the NP surface [63]. In fact, in figure 10, a morphologic examination performed by TEM shows a pluronic layer surrounding PLGA NPs. The surfactant causes steric repulsions forming a mechanic barrier prohibiting droplet approaching. Thermodynamic stabilization can also be considered, due to a loss of configurational entropy of surface adsorbed pluronic when overlapping occurs for approaching droplets [14]. For all those reasons, it can be concluded that the method followed for the preparation of PLGA NPs produced well-stabilized monodisperse nanoparticles.

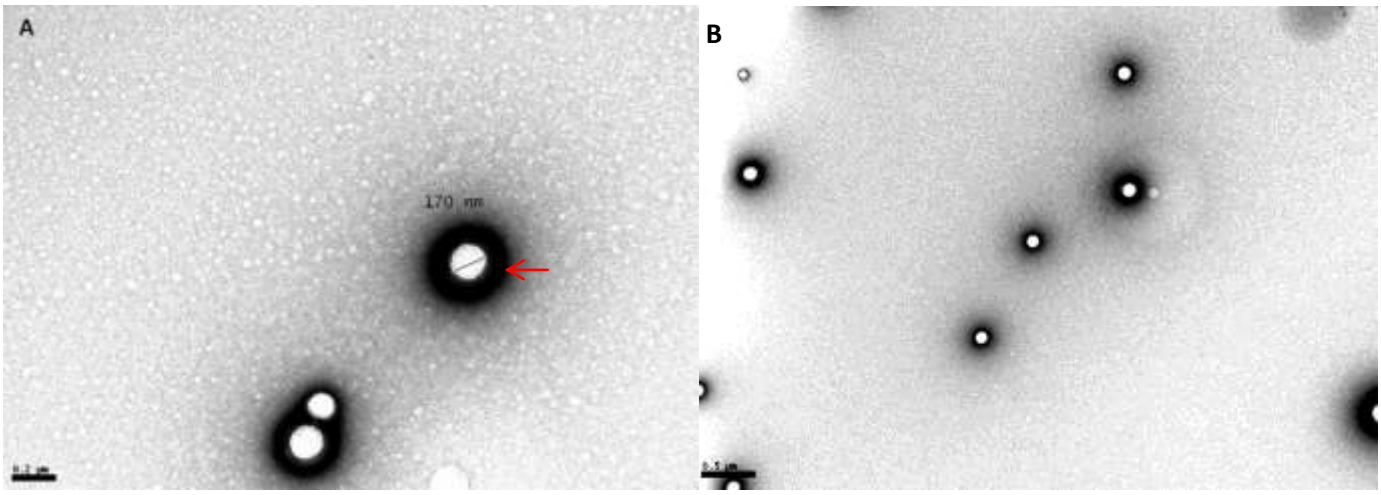

Figure 10 | Transmission electron microscopy images of the: (A) unloaded PLGA nanospheres- the scale bar corresponds to 200 nm; (B) loaded PLGA nanospheres- the scale bar corresponds to 500 nm. The red arrow indicates the pluronic layer surrounding the PLGA NP.

Additionally, TEM analysis of PLGA nanoparticles revealed spherical and uniform shaped nanoparticles, as it is shown in figure 10. The diameter of the nanoparticles revealed by this method changes between approximately 170 and 190 nm, which is in conformity with the size measurement by DLS. These images also show a relatively monodisperse nanoparticles.

The obtained results for encapsulation efficiency for both encapsulated forms of Vitamin D_3 are expressed in percentages in table 5. EE values achieved are according to our experience with other hydrophobic drugs [85] and other results reported in literature that state that EE values for PLGA NPs may vary from 6 to 90% [32]. One reason for not having reached the higher values may be related to vitamin solubility in the surfactant solution [31]. As already reported in other studies, drugs can be incorporated into the core of the micelles formed by Pluronic [34]. As table 5 shows, no significant changes of EE values ($P>0.05$) were

observed for the different cholecalciferol/polymer ratios reported. However for 10% ratios, the attained values significantly decreased (P≤0.05) for the active form of Vitamin D_3, from 83 ± 2% for cholecalciferol to 57 ± 8% for calcitriol. This was already reported by Almouazen and colleagues (2012) [66] and can be explained by cholecalciferol highest hydrophobicity. As calcitriol is less hydrophobic due to the two extra hydroxyl groups, its partition into the aqueous phase may occur during the NPs preparation, resulting in lower EE values.

The cholecalciferol loading capacity of PLGA NPs was also evaluated. As expected, loading capacity values increased significantly (P≤0.05) with the used cholecalciferol/polymer ratio (table 5). Moreover, the produced PLGA NPs, with 10% vitamin/polymer ratio, exhibited significant differences in the determined loading capacity values (P≤0.05). As table 5 shows, cholecalciferol-loaded NPs exhibited a loading capacity of 8.3 ± 0.2%, and the NPs loaded with calcitriol have a loading of 5.7 ± 0.9%. This was already expected due to the decreased encapsulation efficiency values for the active form. PLGA NPs normally exhibit poor loading capacity [32]. Thus, the values obtained in this experimental work are supported by the ones found in the literature as also by our experience with other hydrophobic drugs [85].

The yield of this PLGA NPs production process is quite satisfactory with values of 57 ± 4% (n=3).

4.2 PLGA NPs stability

4.2.1 PLGA NPs stability in liquid phase

Mean diameter, PdI and zeta potential values measured for the purpose of stability tests are presented in table 6. Mean size variation is expressed in terms of ratio S_t/S_i. Cholecalciferol-loaded NPs exhibited a mean S_t/S_i value of 1.031 for approximately 50 days, while calcitriol-loaded presented a value of 1.003. Cholecalciferol- and calcitriol-loaded PLGA NPs showed mean sizes of 199 ± 1 nm and 190 ± 3 nm, respectively, which have remained constant over time. These data proves that the NPs remained physically stable at storage conditions (4 ^{o}C) for approximately 50 days.

Table 6 | Zeta potential, mean diameter and PdI values for both cholecalciferol and calcitriol-loaded PLGA NPs, over a period 60 days, respectively. Mean size variation is expressed in terms of ratio S_t/S_i, where S_f is mean diameter after t days of storage and S_i is the NPs initial mean size. Data represented as mean ± SD (n=3). These data is only relative to one batch for each formulation, loaded and unloaded.

PLGA NPs	Mean diameter (nm)	Ratio S_t/S_i	PdI	Zeta potential (mV)
Cholecalciferol-loaded				
Day 1	199 ± 1	-	0.031 ± 0.014	- 29 ± 1
Day 7	200 ± 3	1.005	0.019 ± 0.017	- 30 ± 1
Day 14	199 ± 3	1.000	0.047 ± 0.006	- 25 ± 1
Day 21	199 ± 5	1.000	0.052 ± 0.016	- 19 ± 1
Day 28	204 ± 4	1.025	0.068 ± 0.017	- 22 ± 1
Day 35	206 ± 4	1.035	0.060 ± 0.021	- 25 ± 1
Day 42	206 ± 5	1.035	0.097 ± 0.020	- 25 ± 5
Day 49	222 ± 6	1.116	0.191 ± 0.034	- 16 ± 1
Day 60	546 ± 100	2.744	0.609 ± 0.113	-10 ± 3
Calcitriol-loaded				
Day 1	190 ± 3	-	0.114 ± 0.029	- 29 ± 2
Day 7	188 ± 1	0.989	0.074 ± 0.036	- 30 ± 1
Day 14	185 ± 1	0.974	0.086 ± 0.030	- 27 ± 1
Day 21	192 ± 6	1.011	0.089 ± 0.026	- 25 ± 2
Day 28	194 ± 1	1.021	0.163 ± 0.032	- 28 ± 1
Day 49	194 ± 6	1.021	0.187 ± 0.052	- 22 ± 3
Day 60	1189 ± 124	6.258	1.000 ± 0.455	-1 ± 1

Zeta potential values showed a slight increase over time (table 6). However as applying an electric field to the sample may alter it, only values for size were considered for stability evaluation purposes.

4.2.2 PLGA NPs stability in solid phase

As the previous results show, the PLGA NPs are stable in aqueous medium only for a certain period of time. Then it was required to find a strategy that will improve their stability. Lyophilization, also known as freeze-drying, is an industrial process which consists on removing water from a frozen sample by sublimation and desorption under vacuum. Freeze-drying cycle can be divided into three steps: freezing, primary drying and secondary drying. In the first step, the liquid suspension is cooled, and ice crystals of pure water forms. Then, the primary drying stage involves sublimation of ice; and the secondary stage, involves the removal of unfrozen

water [94]. DLS measurements were performed to assess the occurrence of aggregation or modification of the PLGA NPs properties after freeze-drying. These data are presented below in table 7.

Table 7 | PLGA NPs physicochemical characterization after freeze-drying experiments, with and without a cryoprotective agent. Mean size variation is expressed in terms of ratio Sf/Si, where Sf is mean diameter after freeze-drying and Si is the NPs initial mean size. Data represented as mean ± SD (n=3).

Cholecalciferol-loaded PLGA NPs	**Mean diameter (nm)**	**Ratio S_f/S_i**	**PdI**	**Zeta potential (mV)**
Before freeze-drying	193 ± 2	-	0.033 ± 0.022	- 28 ± 5
After freeze-drying				
Without cryoprotectants	1573 ± 181	8.108	0.594 ± 0.125	- 27 ± 1
Sucrose 1%	197 ± 14	1.015	0.152 ± 0.050	- 22 ± 1
Calcitriol-loaded PLGA NPs	**Mean diameter (nm)**	**Ratio S_f/S_i**	**PdI**	**Zeta potential (mV)**
Before freeze-drying	186 ± 3	-	0.060 ± 0.010	- 37 ± 2
After freeze-drying				
Without cryoprotectants	1591 ± 167	8.554	0.613 ± 0.369	- 31 ± 1
Sucrose 1%	193 ± 1	1.038	0.096 ± 0.029	- 29 ± 3

The NP mean diameter and PdI values significantly increased ($P \leq 0.05$) after lyophilization without cryoprotectant (table 7). As it is proved by the increased PdI values, freeze-drying process caused PLGA NPs aggregation yielding a polydispersion. No significant changes ($P > 0.05$) were verified for zeta potential values. Hence, it is possible to conclude that these PLGA NPs are not able to overcome the stress caused by the lyophilization process leading to their destabilization and further aggregation. However, these results also demonstrated that 1% sucrose is a cryoprotective agent suitable to preserve particle integrity after reconstitution of lyophilised PLGA nanoparticles, yielding no significant changes in mean diameter ($P > 0.05$). However, zeta potential values suffer a significant decrease in the presence of sucrose ($P \leq 0.05$). This could be explained by sucrose adsorption on NPs surface. The choice of sucrose as the cryoprotective agent was justified by a previous work of Holzer and colleagues that have proven that this is a well suited cryoprotective agent [95]. The action of this agent is essential during the freezing step when a phase separation into ice and cryo-concentrated solution occurs. The cryo-concentrated phase is composed of nanoparticles, free surfactant and unloaded drug. This high concentration of particles induces aggregation. Also, the crystallization of ice exercises a mechanical stress on nanoparticles leading to their destabilization. Though, sucrose creates a glassy matrix and PLGA NPs are imobilizated within

it, preventing their aggregation and protect them against the mechanical stress of ice crystal. For this reason it was concluded that freeze-drying with cryo-protectant agents allows NP stability improvement during storage [94].

UV-VIS measurements demonstrated that vitamin remained stable after this process.

4.3 Calcitriol release from the PLGA nanoparticles

The release profile of calcitriol entrapped in PLGA NPs was carried out in PBS (0.01 M, pH 7.4 at 37 °C). The attained calcitriol release curve is presented in figure 11.

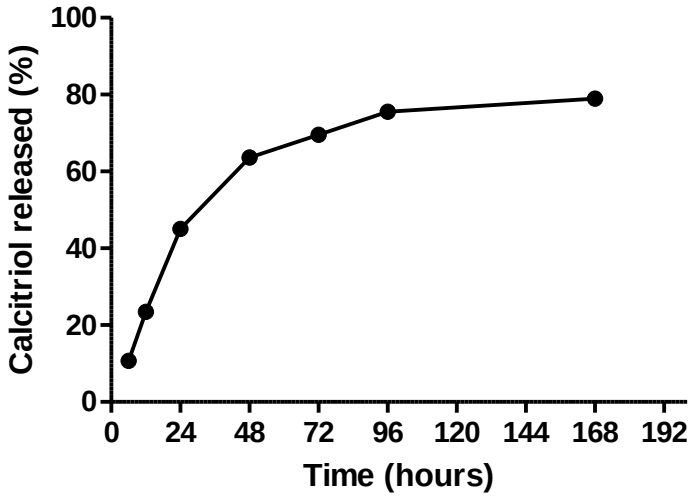

Figure 11| *In vitro* release profile of calcitriol from PLGA NPs in PBS (0.01 M, pH 7.4) at 37 °C.

In vitro drug release testing is an important tool in the quality control of drug delivery systems and it can be used as well for the prediction of *in vivo* drug kinetics. Since drug entrapped in the NPs is not bioavailable, the drug release from nanoparticles is a major determinant in its biological effect. Therefore, assessment of this parameter is very important in these types of systems. The *in vitro* release of drugs from nanocarriers may approximate the physiological drug release profile, mimicking the physiological pH and salt concentrations. PLGA NPs tend to exhibit a biphasic release pattern, characterized by an initial burst release, followed by a slower sustained release [6, 25]. As figure 11 shows, calcitriol released at 24 h was around 45%. This initial rapid release might be attributed to the release of the surface-adsorbed vitamin. The calcitriol entrapped in NPs polymeric matrix was released in a later and more controlled manner, reaching a *quasi-plateau* between 96 and 168 hours. In fact, between fourth and seventh days, only approximately 5% of the encapsulated calcitriol was released. In aqueous medium, PLGA suffers biodegradation by hydrolytic cleavage of its esters linkages into

monomers [4-6, 23-27]. During hydrolysis, acidic degradation products accumulate inside the PLGA NPs and are responsible for reaction auto-catalysis [25, 26]. The hydrolytic breakdown also causes the formation of pores allowing the release of oligomers and monomers, resulting in bulk erosion [23]. Thus, the main pathways for the second phase calcitriol release in PLGA NPs are: drug diffusion through NP matrix, NP matrix hydrolysis and NP erosion [5, 6, 23, 26]. As NPs degradation is slow, the release between 48 and 168 hours may depend mainly of vitamin diffusion through the polymeric matrix and matrix erosion. Therefore features as drug physico-chemical properties and geometry of drug-loaded PLGA NPs (size and shape) exhibit a major impact on the release profile [6, 23, 26]. After 168 hours, the total calcitriol released reached around 80%.

Several studies that developed PLGA NPs for the encapsulation of various drugs have reported this characteristic biphasic release profile from the nanocarriers in PBS at 37 °C [6, 96-98]. These attained results allow concluding that the developed PLGA NPs are an adequate approach for the calcitriol transport and release, due to its biphasic and controlled pattern.

4.4 Cell survival and growth inhibition by calcitriol-loaded NPs

The *in vitro* cytotoxic effects on two pancreatic cancer cell lines, HPNE and S2-013, after treatment with calcitriol entrapped into the prepared PLGA NPs were assessed, comparatively to free calcitriol, in terms of cell survival and growth. Both cells incubated with 0.1% ethanol and bare PLGA NPS during 72 hours had no significant effect on the cell survival (figure 12). The results prove that PLGA nanoparticles are biocompatible, showing no deleterious effects on the viability of the studied cell lines.

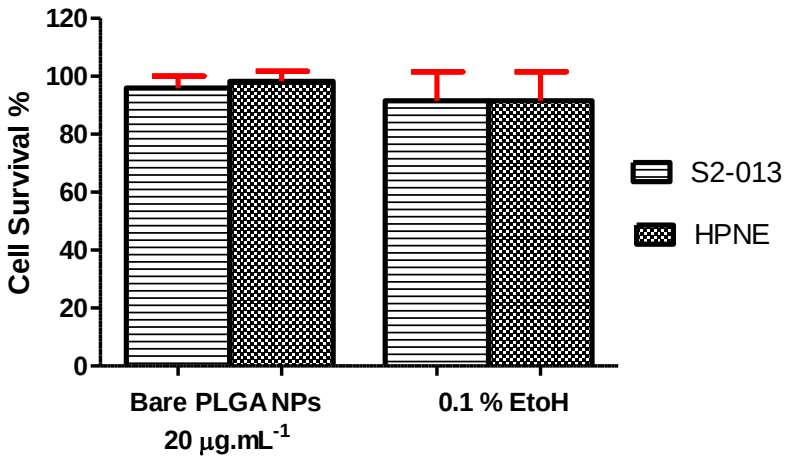

Figure 12 | Cell survival after incubation period in S2-013 and HPNE cell lines. The figures shows data for cells treated with 20 mg.mL^{-1} of bare PLGA NPs and 0.1% ethanol as control. Percent cell survival is expressed relative to that of untreated control cells (null) that did not receive NPs or ethanol. Data represented as mean ± SD (n=3).

The effect of calcitriol at concentrations from 0.005 x 10^3 to 2.5 x 10^3 nM was tested with concentrations of PLGA in the range of 1 x 10^{-1} µg.mL^{-1} to 20 µg.mL^{-1}. From figures 13 to 16 and table 8, the attained results and all the determined values for IC_{50} and GI_{50}, respectively, are presented. It was verified that both free and encapsulated calcitriol exhibit a concentration-related decrease in cell survival and growth in both cell lines (figures 13 and 14). The advantage of PLGA NPs was noticed for both HPNE and S2-013, with calcitriol-NPs being significantly (P≤0.05) more efficient than free calcitriol in inhibiting cell survival and growth (figures 13 and 14). Thus, drug delivery with this polymeric system improves calcitriol antineoplastic activity, resulting in significantly (P≤0.05) lower IC_{50} and GI_{50} values (table 8). For instance in 48 hours assay, free calcitriol inhibits the S2-013 cell growth in 50% when its concentration is of 0.78x10^3 nM (renewed daily, total of 2 administrations resulting in a cumulative concentration of 1.56x10^3 nM), which is about 3 fold higher than equivalent 0.53x10^3 nM calcitriol of the loaded NPs (added only at t=0) which exhibit the same effect (table 8). The GI_{50} results for 48 and 72 hours demonstrate that the total dose of free calcitriol added to the cell lines was 3-3.5 times of the calcitriol NP dose to achieve 50% of cell growth.

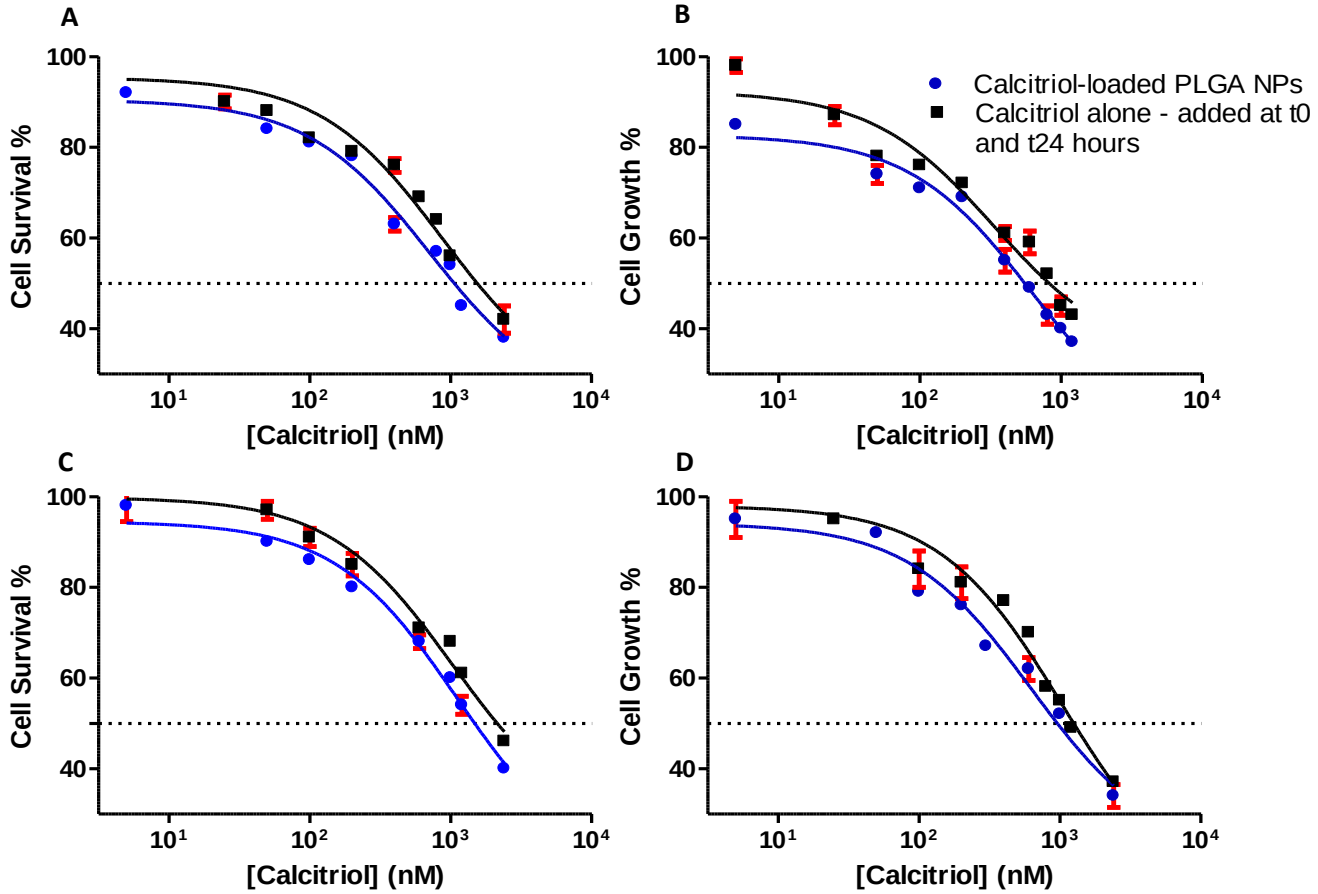

Figure 13| Cytotoxic effects of calcitriol free and entrapped in PLGA NPs after 48 hours treatment on two human pancreatic cell lines, S2-013 (A and B) cells and hTERT-HPNE (C and D), determined by SRB assay. (A) and (C) effects of calcitriol on cell survival; (B) and (D) effects of calcitriol on cell growth. Free calcitriol was supplemented daily due to its short half-life. Survival inhibition is presented as percent [(%)=T/C x 100]; as growth inhibition [(%)=((T-T_0)/(C-T_0)) x 100].

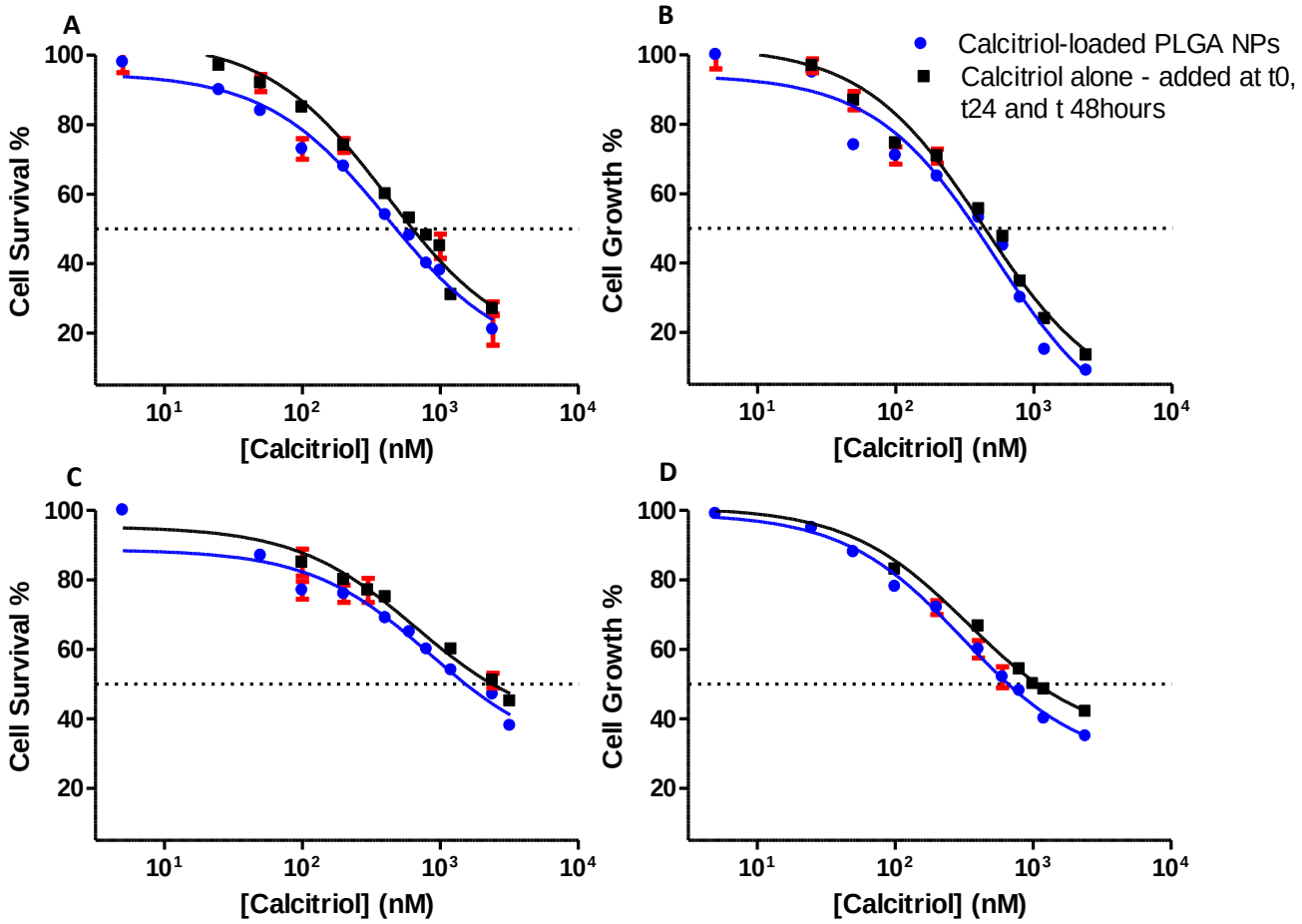

Figure 14 | Cytotoxic effects of calcitriol free and entrapped in PLGA NPs after 72 hours treatment on two human pancreatic cell lines, S2-013 (A and B) cells and hTERT-HPNE (C and D), determined by SRB assay. (A) and (C) effects of calcitriol on cell survival; (B) and (D) effects of calcitriol on cell growth. Free calcitriol was supplemented daily due to its short half-life.

Still, it is important to highlight that due to the calcitriol short half-life, the presented drug concentrations were added daily, unlike calcitriol loaded in NPs that was only added once, at time t0. So, in the 48 hours assay, 2.4 x 10^3 nM calcitriol loaded in PLGA NPs reduced the cell growth of S2-013 cell line to about 15 % compared with 30 % when calcitriol was administered alone at t=0 and t=24 hr (figure 13B). However, due to daily renewal, free calcitriol 2.4 x 10^3 nM corresponds to a cumulative concentration of 4.8 x 10^3 nM at 48 hours (two administrations of 2.4 x 10^3 nM) and 7.2 x 10^3 nM at 72 hours (three administrations of 2.4 x 10^3 nM).

Despite the NPs themselves already show an advantage compared to calcitriol alone renovated daily; if the comparison was made between loaded NPs and single-add free calcitriol instead of renewed daily calcitriol, that advantage would be much more evident as demonstrated by figure 16. As figure 15 depicts, for the same range of concentrations, calcitriol single-added at t=0 shows a decreased *in vitro* anti-tumor activity when comparing

with calcitriol daily renewed, resulting in IC_{50} ($P \leq 0.05$) value of 2.19 x 10^3 nM, compared to 2 administrations of calcitriol (1.51 x 10^3 nM) in 48 hours (calcitriol total= 3.02 x 10^3 nM) to achieve the same effect. Thus, to use low calcitriol concentrations for comparing the efficacy of the calcitriol loaded NPs, free calcitriol daily renovation was performed in all assays.

Due to calcitriol short half-life, daily renewal was necessary to maintain the concentration of vitamin D, increasing the frequency of administration and consequently use more drug than in the case of vitamin encapsulated in the PLGA nanoparticles. As a result, the obtained data prove that PLGA NPs enhance calcitriol antineoplasic activity, allowing reducing the administration frequency, as well to use low doses of drug.

Table 8 | Cytotoxic effects of calcitriol on the survival and growth of both cell lines, S2-013 and HPNE, respectively. Results are expressed as IC_{50} and GI_{50} at 48 and 72 hours of exposure with calcitriol free and entrapped in PLGA NPs by SRB assay. Free calcitriol was supplemented daily to its short half-life.

	IC50 (10^3nM)		**GI50 (10^3nM)**	
48 hours assay	**S2-013**	**hTERT-HPNE**	**S2-013**	**hTERT-HPNE**
Calcitriol (renewed daily)	1.51 ± 0.05	1.95 ± 0.03	0.78 ± 0.01	1.25 ± 0.01
Calcitriol loaded-PLGA NPs	1.10 ± 0.06	1.46 ± 0.05	0.53 ± 0.02	1.12 ± 0.04
72 hours assay				
Calcitriol (renewed daily)	0.61 ± 0.01	1.63 ± 0.01	0.48 ± 0.01	1.08 ± 0.01
Calcitriol loaded-PLGA NPs	0.52 ± 0.01	1.22 ± 0.01	0.43 ± 0.01	0.83 ± 0.02

The benefits of NPs could be explained by the efficient cell internalization of PLGA NPs as due to their rapid endo-lysosomal escape already reported by Panyam and co-workers [99]. It is expected an improvement of the intracellular delivery of encapsulated vitamin compared to the free one. This can be attributed to the fact that NPs may have been more readily internalized by an endocytosis mechanism [100], while free calcitriol may have been transported into cells by a passive diffusion mechanism, suggesting that the multi-drug resistance problem, effluxing of calcitriol out of cells by p-glycoprotein pump existing within cell membrane, might be circumvented by the nanoparticle approach [30, 100]. The efficient uptake of PLGA-NPs by S2-013 and hTERT-HPNE cells has been previously reported before by our group [85]. Also, despite calcitriol having a short half-life, its entrapment in PLGA NPs

allows vitamin protection, sustained and controlled delivery, avoiding drug degradation and inactivation.

For both cell types, treatment with encapsulated and non-encapsulated calcitriol for 72 hours had shown significantly (P≤0.05) more deleterious effects than 48 hours treatment. The sustained and controlled release of these PLGA NPs explain the attained results of calcitriol loaded NPs in terms of cell survival and cell growth after 48 and 72 hours (figures 13 and 14). From these results, our conclusion is that a longstanding treatment presents more pronounced deleterious effect since these NPs are able to maintain drug concentrations. Also, it is quite relevant to analyze and compare the effect of free calcitriol and loaded NPs on hTERT -HPNE and S2-013 cell lines. The results shown in figures 13 and 14 demonstrated that the calcitriol deleterious effect is significantly (P≤0.05) higher in the cancer cell line, S2-013. IC_{50} and GI_{50} values for S2-013 cells are almost two fold higher than for hTERT –HPNE cells (table 8). Although the NPs potentiate the drug's effect on the HPNE cell line likewise as for the pancreatic tumor cells, HPNE cells show more resistance to vitamin's toxicity, whether calcitriol is encapsulated or not. For instance, while 50 nM calcitriol loaded in PLGA NPs reduce the cell growth of S2-013 cell line to about 80% after 48 hours, at the same concentration calcitriol-PLGA NPs do not show toxicity in the HPNE cell line (figure 13B and 13D).

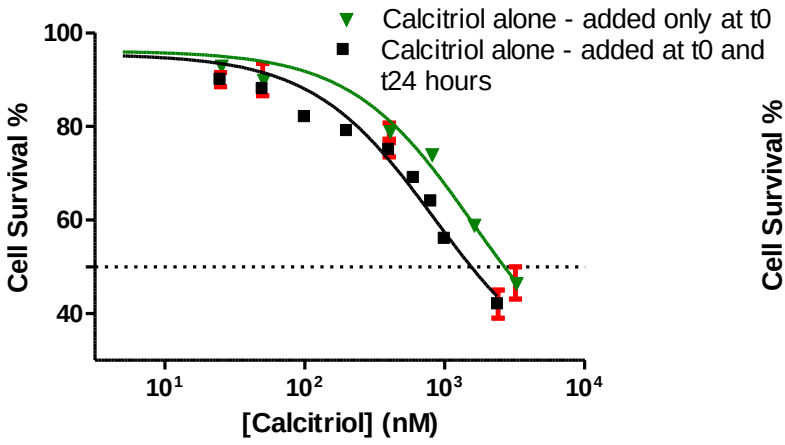

Figure 15 | Effects on cell survival of calcitriol free, single-add and renewed daily, after 48 hours treatment on S2-013 cell line, determined by SRB assay. Survival inhibition is presented as percent [(%)=T/C x 100].

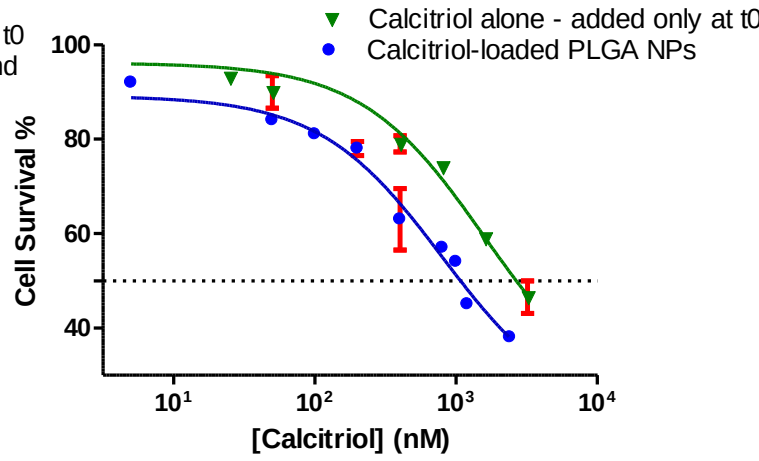

Figure 16 | Effects on cell survival of calcitriol free (single-add) and entrapped in PLGA NPs, after 48 hours treatment on S2-013 cell line, determined by SRB assay. Survival inhibition is presented as percent [(%)=T/C x 100].

5. CONCLUDING REMARKS AND FUTURE PERSPECTIVES

Cancer is the main cause of death worldwide and its conventional therapy has several limitations since anticancer drugs act indiscriminately on both tumor and healthy tissues. Nanoparticles are promising candidates for anticancer drugs delivery, as they present numerous advantages over conventional chemotherapy such as improving the drug water solubility, protecting it from the macrophage uptake, thus enhancing the blood circulation time, and finally providing an increased and controlled release into the specific final target.

Calcitriol, the active metabolite of Vitamin D_3, is a potential anticancer agent. Although as other chemotherapeutic drugs, the use of Vitamin D_3 also exhibits several drawbacks. These limitations are recently leading to numerous investigations in order to design and develop an ideal formulation for Vitamin D_3 delivery to cancer cells. Although significant progress has been made, an ideal carrier has not yet been achieved.

PLGA is one of the most promising biomaterials due to being biocompatible, biodegradable and FDA-approved, and having adjustable biodegradation rate and tunable mechanical properties. Its special features allow protection of drug from degradation and sustained release delivery. For these reasons, in this work, PLGA NPs were proposed to calictriol delivery to cancer cells.

Calcitriol-loaded PLGA NPs were prepared by a single emulsion solvent evaporation method and stabilized with Pluronic F127. Formulation parameters were studied and discussed using cholecalciferol as a drug model to select the NP that presents adequate physicochemical characteristics for the calcitriol encapsulation and delivery into pancreatic cells. The studied formulation parameters were the vitamin/polymer ratio and sonication time. The prepared PLGA NPs exhibit a spherical shape, mean diameter ranging between 170 and 190 nm, low PdI values and negative zeta potential values. While cholecalciferol entrapment reached values of efficiency of approximately 83%, for calcitriol loaded-PLGA NPs the attained encapsulation efficiency values were lower (57%). The prepared NPs exhibited loading capacity values in the order of 5-8% and a process yield of about 57%. The prepared system is stable at storage conditions for several weeks and was lyophilized to increase its shelf-life. 1% sucrose was a cryoprotective agent suitable to preserve particle integrity after reconstitution of lyophilised drug-loaded PLGA nanoparticles.

The prepared PLGA nanoparticles exhibited a biphasic release profile, as reported before in several published studies that developed PLGA NPs for the encapsulation of several drugs. Approximately 45% of calcitriol was released in the first 24 hours, which may be

correspondent to the surface-adsorbed vitamin. This burst release was followed by a slower sustained release phase, attributed to the calcitriol entrapped in the NPs polymeric matrix, reaching approximately 80% of released calcitriol after 7 days.

The *in vitro* cytotoxic studies proved that bare PLGA NPs are biocompatible and also revealed that this nanosystem allowed maintaining and enhancing the antineoplastic effect of calcitriol against human pancreatic cancer cells. Moreover this system provides drug protection and prevention from degradation, increasing calcitriol half-life. Besides the enhanced drug bioavailability, this formulation may have better selectivity for target cancer cells and tissues, since, in a certain concentration range, calcitriol-NPs exhibit deleterious effects on the cancer cells, but not in the healthy cells.

All these results suggest that the obtained nanoparticles could be good candidates for vitamin D_3 release to animals and humans. Thus, we can also conclude that nanoencapsulation in PLGA NPs may offer a new and potentially effective administration strategy of calcitriol that overcomes the actual limitations as its bioavailability and toxicity.

5.1 Future perspectives

Several assays and experiments could have been conducted to upgrade the developed system as to improve its characterization, but were not possible to perform due to time restrictions and experimental problems. Although, the prepared PLGA nanoparticles have proved to be a promising new approach to calcitriol delivery to cancer cells, further development is required. For instance surface modification, with specific biomolecules or antibodies, may improve their targeting and accumulation in target-tissue as increase their bioavailability.

Finally, *in vivo* tests using animal models, as pharmacokinetics and biodistribution studies would be interesting to evaluate in detail the system efficacy. However these studies would entail a costly investment.

REFERENCES

1. Jemal, A., F. Bray, M.M. Center, J. Ferlay, E. Ward, and D. Forman, *Global cancer statistics.* CA Cancer J Clin, 2011. **61**(2): p. 69-90.
2. Brannon-Peppas, L. and J.O. Blanchette, *Nanoparticle and targeted systems for cancer therapy.* Adv Drug Deliv Rev, 2004. **56**(11): p. 1649-59.
3. Krishnan, A.V. and D. Feldman, *Mechanisms of the anti-cancer and anti-inflammatory actions of vitamin D.* Annu Rev Pharmacol Toxicol, 2011. **51**: p. 311-36.
4. Acharya, S. and S.K. Sahoo, *PLGA nanoparticles containing various anticancer agents and tumour delivery by EPR effect.* Adv Drug Deliv Rev, 2011. **63**(3): p. 170-83.
5. Makadia, H.K. and S.J. Siegel, *Poly Lactic-co-Glycolic Acid (PLGA) as Biodegradable Controlled Drug Delivery Carrier.* Polymers (Basel), 2011. **3**(3): p. 1377-1397.
6. Kumari, A., S.K. Yadav, and S.C. Yadav, *Biodegradable polymeric nanoparticles based drug delivery systems.* Colloids Surf B Biointerfaces, 2010. **75**(1): p. 1-18.
7. Steichen, S.D., M. Caldorera-Moore, and N.A. Peppas, *A review of current nanoparticle and targeting moieties for the delivery of cancer therapeutics.* European Journal of Pharmaceutical Sciences, 2013. **48**(3): p. 416-427.
8. Kawasaki, E.S. and A. Player, *Nanotechnology, nanomedicine, and the development of new, effective therapies for cancer.* Nanomedicine, 2005. **1**(2): p. 101-9.
9. Semete, B., L. Booysen, Y. Lemmer, L. Kalombo, L. Katata, J. Verschoor, and H.S. Swai, *In vivo evaluation of the biodistribution and safety of PLGA nanoparticles as drug delivery systems.* Nanomedicine : nanotechnology, biology, and medicine, 2010. **6**(5): p. 662-671.
10. Wang, M. and M. Thanou, *Targeting nanoparticles to cancer.* Pharmacol Res, 2010. **62**(2): p. 90-9.
11. Parhi, P., C. Mohanty, and S.K. Sahoo, *Nanotechnology-based combinational drug delivery: an emerging approach for cancer therapy.* Drug Discov Today, 2012. **17**(17-18): p. 1044-52.
12. Liu, Y., H. Miyoshi, and M. Nakamura, *Nanomedicine for drug delivery and imaging: a promising avenue for cancer therapy and diagnosis using targeted functional nanoparticles.* Int J Cancer, 2007. **120**(12): p. 2527-37.
13. Brigger, I., C. Dubernet, and P. Couvreur, *Nanoparticles in cancer therapy and diagnosis.* Advanced Drug Delivery Reviews, 2012. **64, Supplement**(0): p. 24-36.
14. Wilczewska, A.Z., K. Niemirowicz, K.H. Markiewicz, and H. Car, *Nanoparticles as drug delivery systems.* Pharmacol Rep, 2012. **64**(5): p. 1020-37.
15. Byrne, J.D., T. Betancourt, and L. Brannon-Peppas, *Active targeting schemes for nanoparticle systems in cancer therapeutics.* Adv Drug Deliv Rev, 2008. **60**(15): p. 1615-26.
16. Zhang, L., F.X. Gu, J.M. Chan, A.Z. Wang, R.S. Langer, and O.C. Farokhzad, *Nanoparticles in medicine: therapeutic applications and developments.* Clin Pharmacol Ther, 2008. **83**(5): p. 761-9.
17. Haley, B. and E. Frenkel, *Nanoparticles for drug delivery in cancer treatment.* Urol Oncol, 2008. **26**(1): p. 57-64.
18. Wang, A.Z., R. Langer, and O.C. Farokhzad, *Nanoparticle delivery of cancer drugs.* Annu Rev Med, 2012. **63**: p. 185-98.
19. Dan, P., M.K. Jeffrey, H. Seungpyo, C.F. Omid, M. Rimona, and L. Robert, *Nanocarriers as an emerging platform for cancer therapy.* Nature Nanotechnology, 2007. **2**(12): p. 751-760.
20. Ye, L., J. He, Z. Hu, Q. Dong, H. Wang, F. Fu, and J. Tian, *Antitumor effect and toxicity of Lipusu in rat ovarian cancer xenografts.* Food and Chemical Toxicology, 2013. **52**(0): p. 200-206.

21. Bawa, R., *Nanoparticle-Based Therapeutics in Humans: A Survey.* Nanotech. L. & Bus., 2008. **5**(2): p. 135-155.
22. Brahmachari, B., A. Hazra, and A. Majumdar, *Adverse drug reaction profile of nanoparticle versus conventional formulation of paclitaxel: An observational study.* Indian J Pharmacol, 2011. **43**(2): p. 126-30.
23. Cohen, S., T. Yoshioka, M. Lucarelli, L.H. Hwang, and R. Langer, *Controlled delivery systems for proteins based on poly(lactic/glycolic acid) microspheres.* Pharm Res, 1991. **8**(6): p. 713-20.
24. Wang, Z., W.K. Chui, and P.C. Ho, *Design of a multifunctional PLGA nanoparticulate drug delivery system: evaluation of its physicochemical properties and anticancer activity to malignant cancer cells.* Pharm Res, 2009. **26**(5): p. 1162-71.
25. Wischke, C. and S.P. Schwendeman, *Principles of encapsulating hydrophobic drugs in PLA/PLGA microparticles.* Int J Pharm, 2008. **364**(2): p. 298-327.
26. Klose, D., F. Siepmann, K. Elkharraz, and J. Siepmann, *PLGA-based drug delivery systems: importance of the type of drug and device geometry.* Int J Pharm, 2008. **354**(1-2): p. 95-103.
27. Santos Jr, A.R. and M. Wada, *Polímeros Biorreabsorvíveis como Substrato para Cultura de Células e Engenharia Tecidual.* Polímeros: Ciência e Tecnologia, 2007. **17**(4): p. 308-317.
28. Kim, S.H., J.H. Jeong, K.W. Chun, and T.G. Park, *Target-specific cellular uptake of PLGA nanoparticles coated with poly(L-lysine)-poly(ethylene glycol)-folate conjugate.* Langmuir, 2005. **21**(19): p. 8852-7.
29. Zheng, Y., B. Yu, W. Weecharangsan, L. Piao, M. Darby, Y. Mao, R. Koynova, X. Yang, H. Li, S. Xu, L.J. Lee, Y. Sugimoto, R.W. Brueggemeier, and R.J. Lee, *Transferrin-conjugated lipid-coated PLGA nanoparticles for targeted delivery of aromatase inhibitor 7alpha-APTADD to breast cancer cells.* Int J Pharm, 2010. **390**(2): p. 234-41.
30. Vasir, J.K. and V. Labhasetwar, *Biodegradable nanoparticles for cytosolic delivery of therapeutics.* Adv Drug Deliv Rev, 2007. **59**(8): p. 718-28.
31. Hans, M.L.L., A.M., *Biodegradable nanoparticles for drug delivery and targeting.* Current Opinion in Solid State and Materials Science, 2002. **6**: p. 319-327.
32. Danhier, F., E. Ansorena, J.M. Silva, R. Coco, A. Le Breton, and V. Preat, *PLGA-based nanoparticles: an overview of biomedical applications.* J Control Release, 2012. **161**(2): p. 505-22.
33. Schubert, S., J.J.T. Delaney, and U.S. Schubert, *Nanoprecipitation and nanoformulation of polymers: from history to powerful possibilities beyond poly(lactic acid).* Soft Matter, 2011. **7**(5): p. 1581-1588.
34. Fessi, H., F. Puisieux, J.P. Devissaguet, N. Ammoury, and S. Benita, *Nanocapsule formation by interfacial polymer deposition following solvent displacement.* International Journal of Pharmaceutics, 1989. **55**(1): p. R1-R4.
35. Rhee, Y.-S.P., Chun-Woong ; DeLuca, Patrick P.; Mansour, Heidi M., *Sustained-Release Injectable Drug Delivery.* Pharmaceutical Technology, 2010. **Supplement**: p. 6-13.
36. Agency, E.M. *A Double-Blind, Randomised, Placebo-Controlled, Two-Phase Study (a Single Ascending Dose Phase Followed by a Proof of Concept Phase) to Assess the Safety, Efficacy and Pharmacokinetics of FX005 (50:50 PLGA) Microspheres for the Treatment of Pain in Osteoarthritis of the Knee.* [[online]: https://www.clinicaltrialsregister.eu/ctr-search/trial/2010-022976-29/GB] 2010 29/06/2013 29/06/2013].
37. Moraes, C.M., A.P. de Matos, E. de Paula, A.H. Rosa, and L.F. Fraceto, *Benzocaine loaded biodegradable poly-(d,l-lactide-co-glycolide) nanocapsules: factorial design and characterization.* Materials Science and Engineering: B, 2009. **165**(3): p. 243-246.
38. Dhar, S., F.X. Gu, R. Langer, O.C. Farokhzad, and S.J. Lippard, *Targeted delivery of cisplatin to prostate cancer cells by aptamer functionalized Pt(IV) prodrug-PLGA–PEG*

nanoparticles. Proceedings of the National Academy of Sciences, 2008. **105**(45): p. 17356-17361.
39. Butoescu, N., C.A. Seemayer, M. Foti, O. Jordan, and E. Doelker, *Dexamethasone-containing PLGA superparamagnetic microparticles as carriers for the local treatment of arthritis.* Biomaterials, 2009. **30**(9): p. 1772-1780.
40. Kalaria, D.R., G. Sharma, V. Beniwal, and M.N.V. Ravi Kumar, *Design of Biodegradable Nanoparticles for Oral Delivery of Doxorubicin: In vivo Pharmacokinetics and Toxicity Studies in Rats.* Pharmaceutical Research, 2009. **26**(3): p. 492-501.
41. Snehalatha, M.V., Kolachina ; Saha, Ranendra N. ; Babbar, Anil Kumar; Sharma, Rakesh Kumar, *Etoposide Loaded PLGA and PCL Nanoparticles II: Biodistribution and Pharmacokinetics after Radiolabeling with Tc-99m.* Drug Delivery, 2008. **15**(5): p. 277-287.
42. Lecaroz, M.C., M.J. Blanco-Prieto, M.A. Campanero, H. Salman, and C. Gamazo, *Poly(D,L-lactide-coglycolide) particles containing gentamicin: pharmacokinetics and pharmacodynamics in Brucella melitensis-infected mice.* Antimicrob Agents Chemother, 2007. **51**(4): p. 1185-90.
43. Cui, F., K. Shi, L. Zhang, A. Tao, and Y. Kawashima, *Biodegradable nanoparticles loaded with insulin–phospholipid complex for oral delivery: Preparation, in vitro characterization and in vivo evaluation.* Journal of Controlled Release, 2006. **114**(2): p. 242-250.
44. Danhier, F., N. Lecouturier, B. Vroman, C. Jérôme, J. Marchand-Brynaert, O. Feron, and V. Préat, *Paclitaxel-loaded PEGylated PLGA-based nanoparticles: In vitro and in vivo evaluation.* Journal of Controlled Release, 2009. **133**(1): p. 11-17.
45. Acharya, S., F. Dilnawaz, and S.K. Sahoo, *Targeted epidermal growth factor receptor nanoparticle bioconjugates for breast cancer therapy.* Biomaterials, 2009. **30**(29): p. 5737-5750.
46. Pandey, R., A. Zahoor, S. Sharma, and G.K. Khuller, *Nanoparticle encapsulated antitubercular drugs as a potential oral drug delivery system against murine tuberculosis.* Tuberculosis (Edinburgh, Scotland), 2003. **83**(6): p. 373-378.
47. Xiong, S., S. George, H. Yu, R. Damoiseaux, B. France, K.W. Ng, and J.S. Loo, *Size influences the cytotoxicity of poly (lactic-co-glycolic acid) (PLGA) and titanium dioxide (TiO2) nanoparticles.* Arch Toxicol, 2013. **87**(6): p. 1075-86.
48. Holick, M.F., *Vitamin D: its role in cancer prevention and treatment.* Prog Biophys Mol Biol, 2006. **92**(1): p. 49-59.
49. Glade, M.J., *Vitamin D: health panacea or false prophet?* Nutrition, 2013. **29**(1): p. 37-41.
50. Adams, J.S. and M. Hewison, *Update in vitamin D.* J Clin Endocrinol Metab, 2010. **95**(2): p. 471-8.
51. Jones, G., S.A. Strugnell, and H.F. DeLuca, *Current understanding of the molecular actions of vitamin D.* Physiol Rev, 1998. **78**(4): p. 1193-231.
52. Vieth, R., *The Pharmacology of Vitamin D, Including Fortification Strategies*, in *Vitamin D*, D.P. Feldman, J.W.; Glorieux, F.H., Editor. 2005, Elsevier Acad Press: New York. p. 995-1015.
53. Bikle, D.D., *Vitamin D: Production, Metabolism, and Mechanisms of Action*, in *DISEASES OF BONE AND MINERAL METABOLISM*, F. Singer, Editor 2009, Endotext.org: South Dartmouth.
54. Gonnet, M., L. Lethuaut, and F. Boury, *New trends in encapsulation of liposoluble vitamins.* J Control Release, 2010. **146**(3): p. 276-90.
55. Bikle, D.D., *What is new in vitamin D: 2006-2007.* Curr Opin Rheumatol, 2007. **19**(4): p. 383-8.
56. Garland, C.F., E.D. Gorham, S.B. Mohr, and F.C. Garland, *Vitamin D for cancer prevention: global perspective.* Ann Epidemiol, 2009. **19**(7): p. 468-83.

57. Krishnan, A.V., D.L. Trump, C.S. Johnson, and D. Feldman, *The role of vitamin D in cancer prevention and treatment.* Endocrinol Metab Clin North Am, 2010. **39**(2): p. 401-18, table of contents.
58. Deeb, K.K., D.L. Trump, and C.S. Johnson, *Vitamin D signalling pathways in cancer: potential for anticancer therapeutics.* Nat Rev Cancer, 2007. **7**(9): p. 684-700.
59. Trump, D.L., K.K. Deeb, and C.S. Johnson, *Vitamin D: considerations in the continued development as an agent for cancer prevention and therapy.* Cancer J, 2010. **16**(1): p. 1-9.
60. Beer, T.M. and A. Myrthue, *Calcitriol in cancer treatment: from the lab to the clinic.* Mol Cancer Ther, 2004. **3**(3): p. 373-81.
61. Kawa, S., T. Nikaido, Y. Aoki, Y. Zhai, T. Kumagai, K. Furihata, S. Fujii, and K. Kiyosawa, *Vitamin D analogues up-regulate p21 and p27 during growth inhibition of pancreatic cancer cell lines.* Br J Cancer, 1997. **76**(7): p. 884-9.
62. Schwartz, G.G., D. Eads, A. Rao, S.D. Cramer, M.C. Willingham, T.C. Chen, D.P. Jamieson, L. Wang, K.L. Burnstein, M.F. Holick, and C. Koumenis, *Pancreatic cancer cells express 25-hydroxyvitamin D-1 alpha-hydroxylase and their proliferation is inhibited by the prohormone 25-hydroxyvitamin D3.* Carcinogenesis, 2004. **25**(6): p. 1015-26.
63. Wolpin, B.M., K. Ng, Y. Bao, P. Kraft, M.J. Stampfer, D.S. Michaud, J. Ma, J.E. Buring, H.D. Sesso, I.M. Lee, N. Rifai, B.B. Cochrane, J. Wactawski-Wende, R.T. Chlebowski, W.C. Willett, J.E. Manson, E.L. Giovannucci, and C.S. Fuchs, *Plasma 25-hydroxyvitamin D and risk of pancreatic cancer.* Cancer Epidemiol Biomarkers Prev, 2012. **21**(1): p. 82-91.
64. Chiang, K.C. and T.C. Chen, *Vitamin D for the prevention and treatment of pancreatic cancer.* World J Gastroenterol, 2009. **15**(27): p. 3349-54.
65. Hager, G., M. Formanek, C. Gedlicka, D. Thurnher, B. Knerer, and J. Kornfehl, *1,25(OH)2 vitamin D3 induces elevated expression of the cell cycle-regulating genes P21 and P27 in squamous carcinoma cell lines of the head and neck.* Acta Otolaryngol, 2001. **121**(1): p. 103-9.
66. Almouazen, E., S. Bourgeois, L.P. Jordheim, H. Fessi, and S. Briancon, *Nano-encapsulation of vitamin D3 active metabolites for application in chemotherapy: formulation study and in vitro evaluation.* Pharm Res, 2013. **30**(4): p. 1137-46.
67. Beer, T.M., M. Munar, and W.D. Henner, *A Phase I trial of pulse calcitriol in patients with refractory malignancies.* Cancer, 2001. **91**(12): p. 2431-2439.
68. Nguyen, T.L.U., S.Y. Tey, M.H. Pourgholami, D.L. Morris, T.P. Davis, C. Barner-Kowollik, and M.H. Stenzel, *Synthesis of semi-biodegradable crosslinked microspheres for the delivery of 1,25 dihydroxyvitamin D3 for the treatment of hepatocellular carcinoma.* European Polymer Journal, 2007. **43**(5): p. 1754-1767.
69. Bonor, J.C., R.J. Schaefer, N. Menegazzo, K. Booksh, and A.G. Nohe, *Design of 1,25 dihydroxyvitamin D3 coupled quantum dots, a novel imaging tool.* J Nanosci Nanotechnol, 2012. **12**(3): p. 2185-91.
70. Finlay, I.G., G.J. Stewart, P. Shirley, S. Woolfe, M.H. Pourgholami, and D.L. Morris, *Hepatic arterial and intravenous administration of 1,25-dihydroxyvitamin D3--evidence of a clinically significant hepatic first-pass effect.* Cancer Chemother Pharmacol, 2001. **48**(3): p. 209-14.
71. Kentish, S., T.J. Wooster, M. Ashokkumar, S. Balachandran, R. Mawson, and L. Simons, *The use of ultrasonics for nanoemulsion preparation.* Innovative Food Science & Emerging Technologies, 2008. **9**(2): p. 170-175.
72. Mahdi Jafari, S., Y. He, and B. Bhandari, *Nano-Emulsion Production by Sonication and Microfluidization—A Comparison.* International Journal of Food Properties, 2006. **9**(3): p. 475-485.

73. Li, M., O. Rouaud, and D. Poncelet, *Microencapsulation by solvent evaporation: state of the art for process engineering approaches.* Int J Pharm, 2008. **363**(1-2): p. 26-39.
74. Boyd, R.D., S.K. Pichaimuthu, and A. Cuenat, *New approach to inter-technique comparisons for nanoparticle size measurements; using atomic force microscopy, nanoparticle tracking analysis and dynamic light scattering.* Colloids and Surfaces A: Physicochemical and Engineering Aspects, 2011. **387**(1–3): p. 35-42.
75. Tscharnuter, W., *Photon Correlation Spectroscopy in Particle Sizing*, in *Encyclopedia of Analytical Chemistry*. 2006, John Wiley & Sons, Ltd.
76. Nobbmann, U., M. Connah, B. Fish, P. Varley, C. Gee, S. Mulot, J. Chen, L. Zhou, Y. Lu, F. Shen, J. Yi, and S.E. Harding, *Dynamic light scattering as a relative tool for assessing the molecular integrity and stability of monoclonal antibodies.* Biotechnol Genet Eng Rev, 2007. **24**: p. 117-128.
77. Jiang, J., G. Oberdörster, and P. Biswas, *Characterization of size, surface charge, and agglomeration state of nanoparticle dispersions for toxicological studies.* Journal of Nanoparticle Research, 2009. **11**(1): p. 77-89.
78. Kaszuba, M., J. Corbett, F.M. Watson, and A. Jones, *High-concentration zeta potential measurements using light-scattering techniques.* Philos Trans A Math Phys Eng Sci, 2010. **368**(1927): p. 4439-51.
79. Freire, J., M. Domingues, J. Matos, M. Melo, A. Veiga, N. Santos, and M.R.B. Castanho, *Using zeta-potential measurements to quantify peptide partition to lipid membranes.* European Biophysics Journal, 2011. **40**(4): p. 481-487.
80. Wiersema, P.H., A.L. Loeb, and J.T.G. Overbeek, *Calculation of the electrophoretic mobility of a spherical colloid particle.* Journal of Colloid and Interface Science, 1966. **22**(1): p. 78-99.
81. Williams, D. and C.B. Carter, *The Transmission Electron Microscope*, in *Transmission Electron Microscopy*. 1996, Springer US. p. 3-17.
82. Reimer, L.K., H., *Transmission Electron Microscopy*. 5th ed. Springer Series in Optical Sciences, ed. Springer. Vol. 36. 2008, NY, USA: Springer-Verlag.
83. Parveen, S. and S.K. Sahoo, *Long circulating chitosan/PEG blended PLGA nanoparticle for tumor drug delivery.* European Journal of Pharmacology, 2011. **670**(2–3): p. 372-383.
84. Haschemeyer, R.H.M., R.J., *Negative staining*, in *Principles and Techniques of Electron Microscopy - Biological Applications*, M.A. Hayat, Editor. 1972, Van Nostrand Reinhold Company: NY, USA. p. 110-114.
85. Manuela F. Frasco, G.M.A., Filipe Santos-Silva, Maria do Carmo Pereira, Manuel A. N. Coelho *Transferrin Surface-Modified PLGA Nanoparticles-Mediated Delivery of a Proteasome Inhibitor to Human Pancreatic Cancer Cells.* J Nanopart Res, 2014 submitted.
86. Lee, K.M., H. Yasuda, M.A. Hollingsworth, and M.M. Ouellette, *Notch 2-positive progenitors with the intrinsic ability to give rise to pancreatic ductal cells.* Lab Invest, 2005. **85**(8): p. 1003-12.
87. Iwamura, T., T.C. Caffrey, N. Kitamura, H. Yamanari, T. Setoguchi, and M.A. Hollingsworth, *P-selectin expression in a metastatic pancreatic tumor cell line (SUIT-2).* Cancer Res, 1997. **57**(6): p. 1206-12.
88. Papazisis, K.T., G.D. Geromichalos, K.A. Dimitriadis, and A.H. Kortsaris, *Optimization of the sulforhodamine B colorimetric assay.* J Immunol Methods, 1997. **208**(2): p. 151-8.
89. Voigt, V., *Sulforhodamine B Assay and Chemosensitivity*, R.D. Blumenthal, Editor 2005, Humana Press Inc.: Totowa, NJ.
90. Longo-Sorbello, G.S., G.; Banerjee, D.; Bertin, J., *Cytotoxicity and Cell Growth Assays*, in *Cell and Tissue Culture: Assorted Techniques*2006, Elsevier Science: USA. p. 315-324.

91. Skehan, P., R. Storeng, D. Scudiero, A. Monks, J. McMahon, D. Vistica, J.T. Warren, H. Bokesch, S. Kenney, and M.R. Boyd, *New colorimetric cytotoxicity assay for anticancer-drug screening.* J Natl Cancer Inst, 1990. **82**(13): p. 1107-12.
92. Monks, A., D. Scudiero, P. Skehan, R. Shoemaker, K. Paull, D. Vistica, C. Hose, J. Langley, P. Cronise, A. Vaigro-Wolff, and et al., *Feasibility of a high-flux anticancer drug screen using a diverse panel of cultured human tumor cell lines.* J Natl Cancer Inst, 1991. **83**(11): p. 757-66.
93. Musumeci, T., C.A. Ventura, I. Giannone, B. Ruozi, L. Montenegro, R. Pignatello, and G. Puglisi, *PLA/PLGA nanoparticles for sustained release of docetaxel.* Int J Pharm, 2006. **325**(1-2): p. 172-9.
94. Abdelwahed, W., G. Degobert, S. Stainmesse, and H. Fessi, *Freeze-drying of nanoparticles: Formulation, process and storage considerations.* Advanced Drug Delivery Reviews, 2006. **58**(15): p. 1688-1713.
95. Holzer, M., V. Vogel, W. Mantele, D. Schwartz, W. Haase, and K. Langer, *Physico-chemical characterisation of PLGA nanoparticles after freeze-drying and storage.* Eur J Pharm Biopharm, 2009. **72**(2): p. 428-37.
96. Blanco, M.D. and M.J. Alonso, *Development and characterization of protein-loaded poly(lactide-co-glycolide) nanospheres.* European Journal of Pharmaceutics and Biopharmaceutics, 1997. **43**(3): p. 287-294.
97. Park, J., P.M. Fong, J. Lu, K.S. Russell, C.J. Booth, W.M. Saltzman, and T.M. Fahmy, *PEGylated PLGA nanoparticles for the improved delivery of doxorubicin.* Nanomedicine: Nanotechnology, Biology and Medicine, 2009. **5**(4): p. 410-418.
98. Ramchandani, M. and D. Robinson, *In vitro and in vivo release of ciprofloxacin from PLGA 50:50 implants.* Journal of Controlled Release, 1998. **54**(2): p. 167-175.
99. Panyam, J., W.Z. Zhou, S. Prabha, S.K. Sahoo, and V. Labhasetwar, *Rapid endo-lysosomal escape of poly(DL-lactide-co-glycolide) nanoparticles: implications for drug and gene delivery.* FASEB J, 2002. **16**(10): p. 1217-26.
100. Panyam, J. and V. Labhasetwar, *Biodegradable nanoparticles for drug and gene delivery to cells and tissue.* Adv Drug Deliv Rev, 2003. **55**(3): p. 329-47.

APPENDIX

A – Cholecalciferol calibration curve

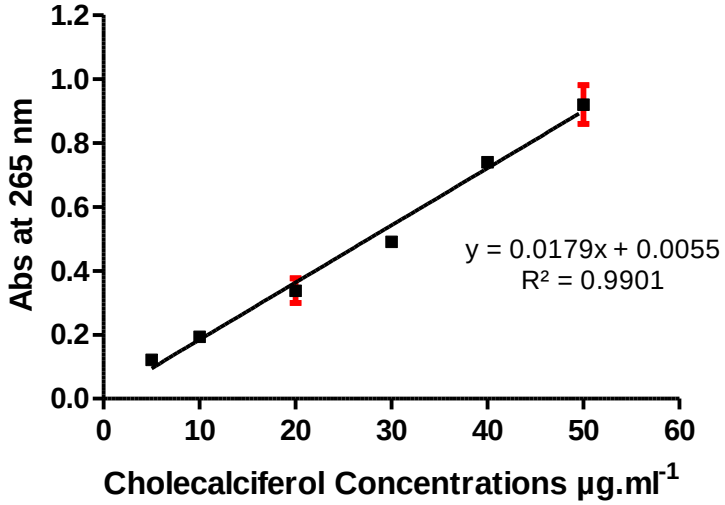

Figure 17 | Cholcalciferoll calibration curve in 3.5% of ethyl acetate in an aqueous solution of 0.1% pluronic. Data vertical lines represent Standard Deviation (n=3).

$$y = (0.0179 \pm 0.0006)\, x + (0.0055 \pm 0.0179)$$

B – Calcitriol calibration curves

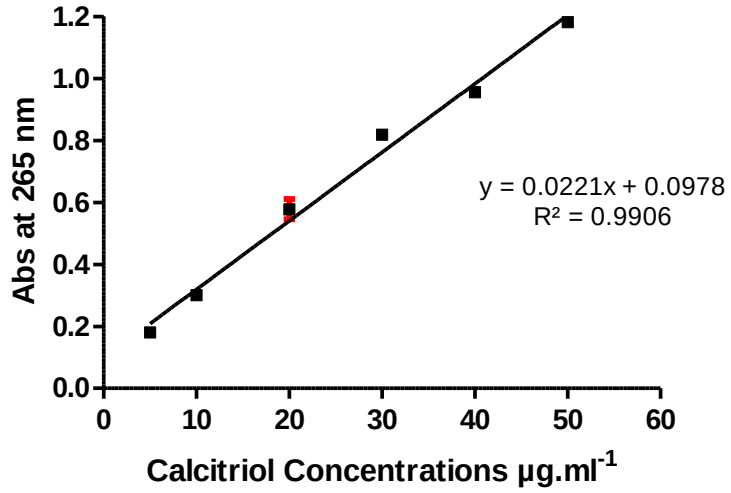

Figure 18| Calcitriol calibration curve in 3.5% of ethyl acetate in an aqueous solution of 0.1% pluronic. Data vertical lines represent Standard Deviation (n=3).

$$\mathrm{y} = (0.0221 \pm 0.0007)\, x + (0.0978 \pm 0.0216)$$

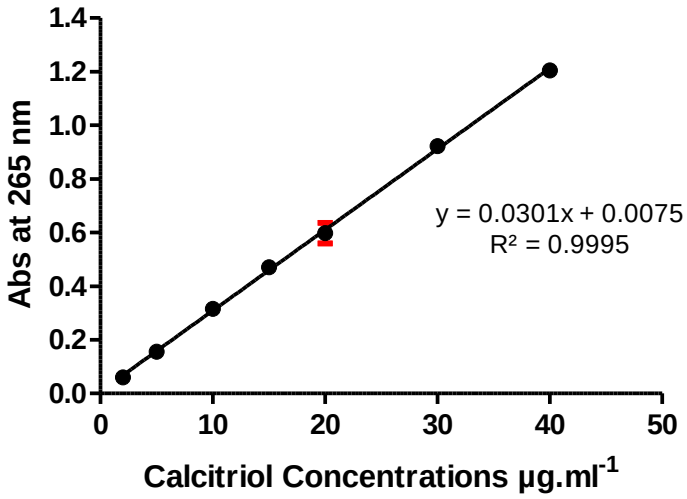

Figure 19| Calcitriol calibration curve in ethanol. Data vertical lines represent Standard Deviation (n=3).

$$y = (0.0301 \pm 0.0003)\, x + (0.0075 \pm 0.0068)$$